

1 **On the contribution of remote sensing-based calibration to model**
2 **multiple hydrological variables in tropical regions**

3 **A. M. Oliveira*** ¹, **A. S. Fleischmann**¹, and **R. C. D. Paiva**¹

4 ¹ Instituto de Pesquisas Hidráulicas (IPH), Universidade Federal do Rio Grande do Sul –
5 UFRGS, Av. Bento Gonçalves, 9500, Porto Alegre 90050-260, RS, Brazil.

6 Corresponding author: Aline Meyer Oliveira (alinemey@gmail.com)

7 **Abstract**

8 The accuracy of hydrological model predictions is limited by uncertainties in model
9 structure and parameterization, and observations used for calibration, validation and
10 model forcing. While calibration is usually performed with discharge estimates, the
11 internal model processes might be misrepresented, and the model might be getting the
12 “right results for the wrong reasons”, thus compromising model reliability. An
13 alternative is to calibrate model parameters with remote sensing (RS) observations of
14 the water cycle. Previous studies highlighted the potential of RS-based calibration to
15 improve discharge estimates, focusing less on other variables of the water cycle. In this
16 study, we analyzed in detail the contribution of five RS-based variables (water level (h),
17 flood extent (A), terrestrial water storage (TWS), evapotranspiration (ET) and soil
18 moisture (W)) to calibrate a coupled hydrologic-hydrodynamic model for a large
19 Amazon sub-basin with extensive floodplains. Single-variable calibration experiments
20 with all variables were able to improve discharge KGE from around 6.1% to 52.9%
21 when compared to a priori parameter sets. Water cycle representation was improved
22 with multi-variable calibration: KGE for all variables were improved in the evaluation
23 period. By analyzing different calibration setups, a consistent selection of

*Present address: Department of Geography, University of Zurich, Zurich, Switzerland.

24 complementary variables for model calibration resulted in a better performance than
25 incorporating all RS variables into the calibration. By looking at multiple RS
26 observations of the water cycle, inconsistencies in model structure and parameterization
27 were found, which would remain unknown if only discharge observations were
28 considered.

29 **Keywords:** hydrological modeling, multi-variable calibration, Amazon, hydrodynamic
30 modeling, large basins.

31

32 **1 Introduction**

33 The accurate representation of hydrologic processes in mathematical models remains a
34 key challenge in water resources research and applications (Baroni et al., 2019; Clark et
35 al., 2015; Kirchner, 2006; Nearing et al., 2016; Semenova & Beven, 2015) due to
36 uncertainties in model structure (Wagener et al., 2003), parameterization (Gharari et al.,
37 2014; Shafii & Tolson, 2015), and observations (Di Baldassarre & Montanari, 2009).
38 These uncertainties might lead to inaccurate predictions of hydrological variables for
39 water resources and natural hazards management (Grimaldi et al., 2019; Montanari &
40 Koutsoyiannis, 2014), and for quantification of impacts of climate change and
41 anthropogenic effects on the water cycle (Haddeland et al., 2006; Teutschbein &
42 Seibert, 2012; C. Y. Xu et al., 2005). This problem has led for instance to initiatives to
43 better constrain the terrestrial water budget by fusing models and Earth Observation
44 datasets (M. Pan & Wood, 2006; Pellet et al., 2019).

45 Traditionally, hydrological models are calibrated against gauged streamflow data, which
46 might hamper predictions in ungauged sites, since it does not guarantee an accurate

47 representation of other water cycle components (e.g., soil moisture and
48 evapotranspiration), thus leading to uncertainty in hydrologic predictions (Hrachowitz et
49 al., 2013). Moreover, many parameter sets can provide equally acceptable performances
50 for streamflow evaluation (i.e., the equifinality thesis), but they might be “right for the
51 wrong reasons” (Beven, 2006; Kirchner, 2006). Several solutions have been proposed to
52 improve process representation and reduce uncertainty in model predictions, such as the
53 generalized likelihood uncertainty estimation (Beven & Binley, 1992), dynamic
54 identifiability analysis (Wagner et al., 2003), multiscale parameter regionalization
55 (Samaniego et al., 2010), and multi-objective calibration (Yapo et al., 1998). However,
56 these are ongoing developments, and stand out as one of the twenty-three unsolved
57 problems in hydrology (Blöschl et al., 2019): “how can we disentangle and reduce
58 model structural/parameter/input uncertainty in hydrological prediction?”.

59 In addition to the presented solutions, an alternative is the use of complementary
60 datasets besides streamflow observations for model calibration (e.g., Crow et al., 2003;
61 Franks et al., 1998; Lo et al., 2010; López et al., 2017; Rajib et al., 2016), data
62 assimilation (e.g., Brêda et al., 2019; Houser et al., 1998; Mitchell et al., 2004; Paiva et
63 al., 2013; Pathiraja et al., 2016; Reichle et al., 2002; Vrugt et al., 2005), or validation
64 (e.g., Alkama et al., 2010; Motovilov et al., 1999; Neal et al., 2012; Siqueira et al.,
65 2018). Such approaches are promising to improve representation of processes in
66 hydrological models (Clark et al., 2015), reduce uncertainty in hydrological predictions
67 (Gharari et al., 2014), understand equifinality (Beven, 2006), and perform predictions in
68 ungauged or poorly-gauged sites (Sivapalan et al., 2003). However, distributed data of
69 complementary hydrological variables (e.g., evapotranspiration, soil moisture) are
70 scarce, and in-situ measurements present poor spatial and temporal representativeness.

71 In this context, remote sensing (RS) observations have stood out in the last decade
72 because of their increasing spatial and temporal resolutions, free availability in many
73 cases, and capability to record less monitored hydrological variables such as soil
74 moisture, evapotranspiration, and terrestrial water storage (Lettenmaier et al., 2015). For
75 instance, GRACE mission provided monthly estimates of changes in water storage on a
76 global coverage with an accuracy of 2 cm when uniformly estimated over land and
77 oceans (Tapley et al., 2004). Missions such as SMOS, SMAP, AMSR-E and ASCAT
78 were estimated to provide soil moisture data with a median RMSE of 0.06-0.10 m³/m³
79 for the CONUS (Karthikeyan et al., 2017). Altimeters such as Envisat, Jason-2 and
80 ICESat-1 and ICESat-2 can yield water level data with an accuracy ranging from 0.04 m
81 to 0.42 m, involving trade-offs between temporal resolution from 10 to 91 days, and
82 cross-track separation from 15 to 315 km (Jarihani et al., 2013), while the future SWOT
83 mission will provide at least one water level measurement every 21 days for global
84 rivers wider than 100 m (Biancamaria et al., 2016).

85 Although previous studies have analyzed the value of integrating RS data into
86 hydrological modeling through calibration or data assimilation (see review by Xu et al.,
87 2014 and Jiang & Wang, 2019), this topic has not been fully explored to its potential
88 yet. Therefore, in section 1.1, we present major knowledge gaps in the context of RS-
89 based calibration of hydrological models through an extensive literature review. In
90 section 1.2, we describe the aims and contributions of this study.

91

92 **1.1 Literature review on calibration of hydrological models with RS data**

93 A comprehensive, yet non-exhaustive literature review of studies that used RS datasets
94 for parameter estimation in hydrological models is presented in this section and

95 summarized in Figure 1. A total of 62 research articles was found (Supplementary
96 Material Table S1). Most publications involved large study areas ($> 1000 \text{ km}^2$), which is
97 expected because of the usual coarse resolution of RS products. Most studies used RS-
98 derived evapotranspiration for model calibration, followed by soil moisture (Figure 1b),
99 but there were also attempts for calibration of up to eight different RS-derived variables
100 (Nijzink et al., 2018). This indicates a still existent knowledge gap regarding which RS-
101 derived variables are more useful for model calibration. Indeed, many recent studies
102 have investigated the added value of RS-derived information to calibrate hydrological
103 models (Figure 1d; Table S1).

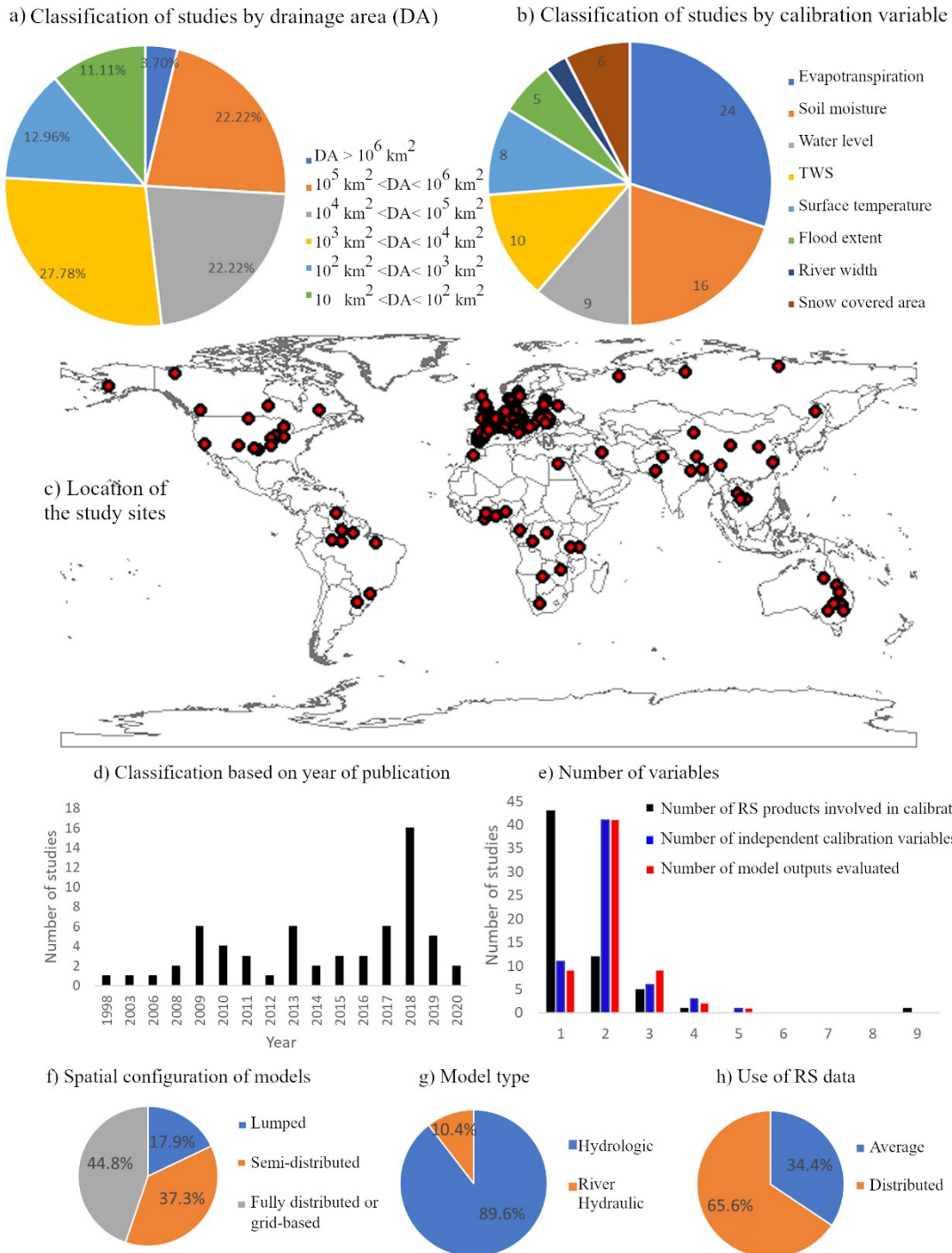
104 Most of the studies (69.35%) used only one RS product for model calibration (Figure
105 1e, in black), while twelve studies (19.35%) used two products, and five (8.06%) used
106 three products. Only few studies used more than three RS products for model
107 calibration (Demirel et al., 2019; Nijzink et al., 2018). Some studies addressed the use
108 of RS data to estimate discharge in ungauged basins (Kittel et al., 2018; Sun et al.,
109 2010), while others focused on narrowing the parameter search space, and thus
110 equifinality reduction, by combining multiple variables for calibration (e.g., Nijzink et
111 al., 2018; Pan et al., 2018). This is confirmed by Figure 1e (in blue), which
112 demonstrates that the vast majority of researches used two variables for calibration (in
113 general, discharge and a RS-derived variable). Within these studies, some analyzed
114 model performance in terms of discharge only, while others considered different
115 variables (Figure 1e, in red), providing a more comprehensive discussion on
116 inconsistencies of hydrological models (e.g., Koch et al., 2018; Li et al., 2018).

117 Regarding how RS is incorporated into the model calibration procedure (Figure 1h),
118 65.6% of the articles used RS-based spatially distributed information, thus calibrating

119 the model with distributed objective functions (e.g., pixel-by-pixel or by sub-basin).
120 Within these studies, bias-insensitive functions have been recently introduced (e.g.,
121 Koch et al., 2018; Demirel et al., 2018; Zink et al., 2018; Dembele et al., 2020), being
122 important for reducing the impact of RS data uncertainty on the parameter estimation
123 procedure. The remaining publications (34.4%) incorporated RS data as an average for
124 the whole basin.

125 Finally, there is still a need for more studies in tropical regions (especially South
126 America) (Figure 1c), which have particular hydro-climatic characteristics, and so have
127 different requirements than temperate regions on model process representation (e.g.,
128 snow-related processes might not be so relevant in some tropical areas, whereas an
129 accurate representation of floodplains might be). In the case of basin with complex
130 river-floodplain interactions as in the Amazon, an accurate flood wave routing method
131 is required to correctly depict the water transport along the drainage network. Our
132 analysis shows that most studies used simple flood wave routing schemes such as
133 kinematic wave or Muskingum (Figure 1g). Only 10.4% attempted to couple hydrologic
134 and river hydrodynamic models, highlighting the necessity of better understanding the
135 applicability of RS-based calibration in basins with major flat regions with wetlands
136 (Hodges, 2013; Neal et al., 2012; Pontes et al., 2017).

137



138

139 **Figure 1.** Summary of the literature review on 62 studies that incorporated RS datasets for
 140 parameter estimation in hydrological models (see Table S1 in Supplementary Material). (a)
 141 Classification of publications based on the drainage area of study sites (an average value was
 142 considered for publications that used multiple study sites); (b) distribution of studies based on
 143 the calibration variable; (c) geographical distribution of study sites; (d) number of publications

144 per year; (e) number of RS products involved in calibration (in black), number of independent
145 calibration variables (in blue), and number of model outputs evaluated (in red); (f) classification
146 of models based on their spatial configuration; (g) model type; and (h) use of RS data

147

148 **1.2 Aims and Contributions of this paper**

149 Our study addresses major knowledge gaps identified in the previous literature review
150 in the context of RS-based calibration of hydrological models. Firstly, most of the
151 studies analyzed two or less variables (Figure 1e). Here, we used RS observations of a
152 large number of variables for model calibration, namely soil moisture,
153 evapotranspiration, terrestrial water storage, flood extent and river water levels, and thus
154 move beyond the contributions of RS for improving only discharge estimates. By
155 simultaneously looking at different variables, we also move towards an improved
156 representation of the water cycle as a whole, enhancing our ability to identify model
157 limitations and inconsistencies. Furthermore, most studies to date focused on European,
158 temperate watersheds (Figure 1c), which largely differ from tropical basins in terms of
159 hydroclimatic characteristics and river-wetland interactions. In this context, large-scale,
160 coupled hydrologic-hydrodynamic models have faced major developments in recent
161 years (Yamazaki et al 2011, Paiva et al 2013, Fleischmann et al 2020), but to our
162 knowledge the complementarity of hydrologic (soil moisture, evapotranspiration,
163 terrestrial water storage) and hydrodynamic (flood extent and river water level) RS
164 observations for model calibration has not yet been addressed in the literature. Here we
165 present a study case in a tropical basin with extensive floodplains in the Amazon with a
166 state-of-the-art coupled hydrologic-hydrodynamic model, which together with the
167 previously mentioned advances provide important contributions to the growing
168 literature of RS-based calibration of hydrological models. This study aims to investigate

169 the applicability of multiple RS observations in an accessible approach to model and
170 represent the water cycle accurately.

171

172 **2 Methods**

173 **2.1 Experimental design**

174 A hydrologic-hydrodynamic model (MGB; (Collischonn et al., 2007)) is set up for a
175 case study in the Amazon (Purus River Basin) with a priori parameter sets based on
176 their variability as reported in literature (references in Table S2). The study is then
177 divided into two steps.

178 Firstly, a sensitivity analysis is performed to understand how different parameter sets
179 (river hydraulic, soil, vegetation) affect model output variables (river discharge, flood
180 extent, river water level, soil moisture, evapotranspiration and terrestrial water storage).

181 Then, a calibration step is performed in which the model is calibrated with the well-
182 known MOCOM-UA optimization algorithm (Yapo et al., (1998)) considering six
183 variables: (1) in-situ streamflow (one gauge at the basin outlet), and RS freely available,
184 state-of-the-art observations of (2) water level (one satellite altimetry virtual station), (3)
185 flood extent (sum of flooded areas over the Lower Purus River Basin), (4) terrestrial
186 water storage (TWS), (5) evapotranspiration, and (6) soil moisture. Variables (4), (5)
187 and (6) are averaged over the whole basin. The calibration of each variable is performed
188 individually (single-variable), and evaluated for all variables. All calibration
189 experiments are repeated three times with differing initial parameter sets to ensure that
190 convergence is not dependent on the initial parameter sets. Given limitations on the
191 availability of simultaneous RS time coverage, the model is calibrated for one time

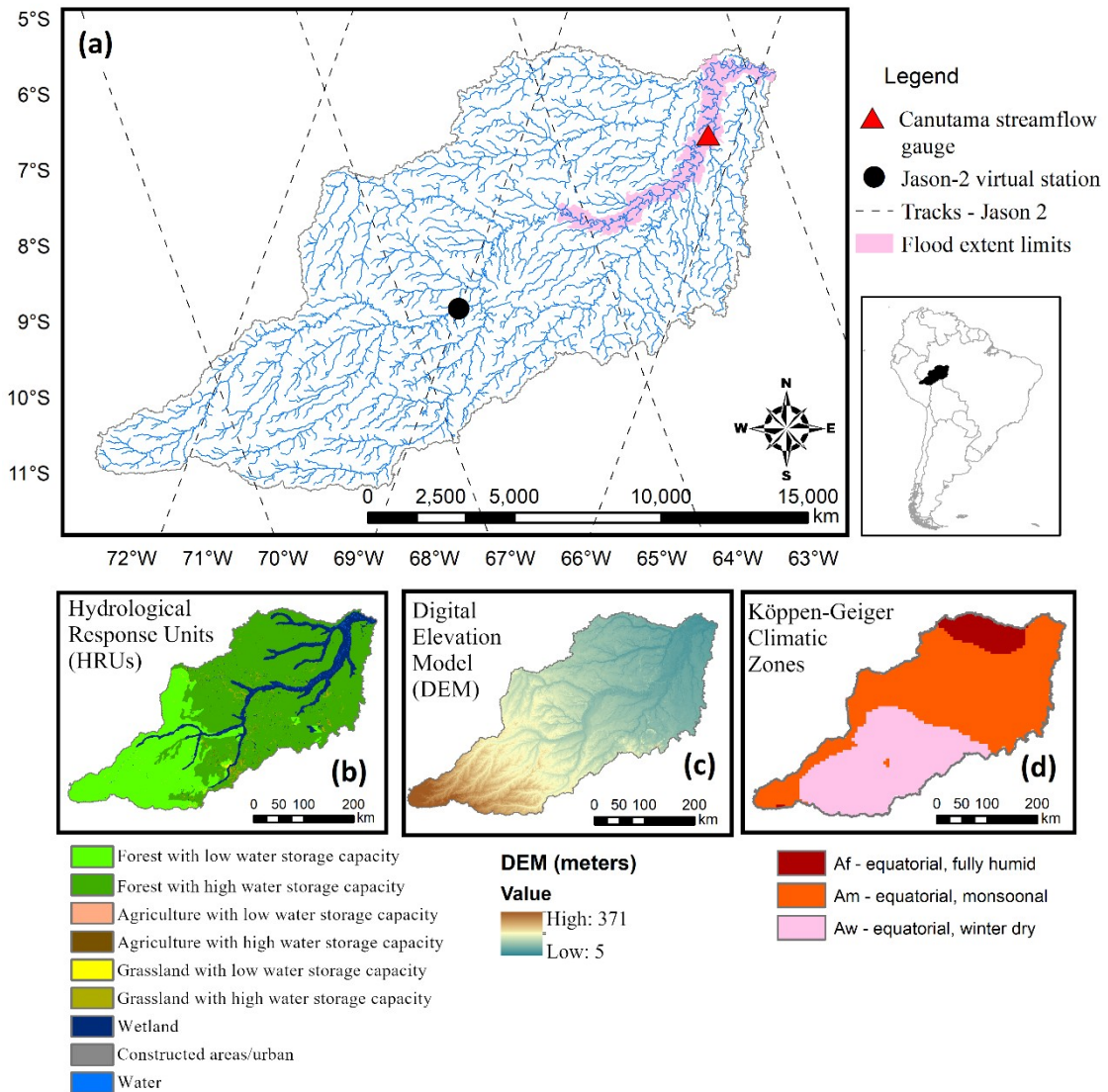
192 period (2009-2011), and evaluated for: (i) the same time period of calibration; and (ii)
193 for a different period (2006–2008 for discharge, flood extent, TWS, ET and 2013–2014
194 for water level and soil moisture). To understand how lumped calibration can retrieve
195 the remotely sensed spatial patterns, a qualitative evaluation is provided additionally. A
196 final test is performed in which two multi-variable calibration experiments are
197 conducted: (i) calibration with all analyzed variables, except discharge; and (ii)
198 calibration with two complementary variables (water level and soil moisture), which are
199 selected for simultaneous calibration for being complementary and having led to
200 satisfactory calibration performance.

201

202 **2.2 Study area: Purus River Basin**

203 The Purus River Basin (Figure 2) in Amazon has a drainage area of approximately
204 236,000 km², and river discharge ranges from around 1,000 (June-December) to 12,000
205 m³/s (January-July) at Canutama gauge. Because of its large area, it is compatible with
206 the spatial resolution of RS products (e.g., a pixel of GRACE presents spatial resolution
207 of roughly 300-400 km). Purus river has minor anthropogenic influences, which
208 simplifies the modeling process. The climate is equatorial (Figure 2d), and mean annual
209 rainfall is 2147 mm/year (according to in-situ gauges). Purus was selected because of its
210 representativeness of tropical regions as the Amazon basin, which is the largest river in
211 the world (Holeman, 1968), and it is characterized by extensive floodplains (Junk,
212 1997). For instance, on the lower Purus, the floodplain width is in the order of 30 km,
213 which corresponds to approximately 30 times the main channel width (Paiva et al.,
214 2011). These floodplains allow a satisfactory flood extent monitoring by RS image
215 classification, which contributes to the suitability of Purus River Basin for this study.

216



217

218 **Figure 2.** Study area: Purus River Basin. (a) drainage network (in blue), location of the
 219 discharge gauge (Canutama, triangle in red), tracks of the spatial altimetry mission Jason 2
 220 (dashed black lines), location of the altimetry virtual station (circle, in black), and the area used
 221 for extraction of flood extent (Lower Purus, pink polygons); (b) Hydrological Response Units
 222 (Fan et al., 2015); (c) Bare Earth Digital Elevation Model (O’Loughlin et al., 2016); (d)
 223 Köppen-Geiger Climatic Zones (Kottek et al., 2006).

224

225 2.3 Hydrologic-hydrodynamic model: MGB

226

227 The MGB (“Modelo de Grandes Bacias”, a Portuguese acronym for “Large Basin
228 Model”) is a semi-distributed, hydrologic-hydrodynamic model (Collischonn et al.,
229 2007; Pontes et al., 2017). It was chosen for this study because (1) it has been widely
230 and successfully applied in several South American basins (e.g., Paiva et al., 2013;
231 Siqueira et al., 2018); (2) it is representative and similar to other conceptual
232 hydrological models like VIC (Liang et al., 1994) and SWAT; and (3) the hydrological
233 component is tightly coupled to a hydrodynamic routing scheme, allowing the
234 simulation of complex flat, tropical basins. Moreover, the source code of MGB is freely
235 available at www.ufrgs.br/lsh.

236 Within the model structure, basins are discretized into unit-catchments, which are
237 further divided into Hydrological Response Units (HRU’s) based on soil type and land
238 use. Model parameters are specific for each of the HRUs. A vertical water balance is
239 performed for each HRU, considering canopy interception, soil infiltration,
240 evapotranspiration, and generation of surface, subsurface and groundwater flows. Soil is
241 represented as a bucket model with a single layer. Flow generated in each HRU is
242 routed to the outlet of the unit-catchment with linear reservoirs. Outflow from each unit-
243 catchment is then propagated through the stream network by using a 1D hydrodynamic
244 model based on the inertial approximation proposed by Bates et al. (2010). The stream
245 network is derived from Digital Elevation Model (DEM) processing. The model has 19
246 parameters, which are further detailed in the next section. Other model inputs are
247 precipitation, climate data, soil type and land use maps, which are further described in
248 section *2.6 Model Setup*.

249

250 **2.4 A priori uncertainty of model parameters**

251

252 Within MGB model, there are parameters related to vegetation cover (albedo, leaf area
253 index, vegetation height and Penman-Monteith surface resistance), river hydraulics
254 (Manning's roughness, and width and depth parameters related to geomorphological
255 relationships), and conceptual parameters related to soil water budget (W_m , b , K_{bas} ,
256 K_{int} , XL , CAP , W_c , CI , CS , CB), which are further detailed in Supplementary Material
257 (Table S2). Out of the 19 model parameters, six are fixed and 13 are calibrated.

258 The a priori uncertainty of MGB model parameters is estimated based on their
259 variability as reported in literature (references in Table S2). Supplementary Material
260 (Table S2) presents the calibration parameters, their initial values, range, and the
261 references that support these assumptions.

262

263 **2.5 Sensitivity analysis**

264

265 In order to understand how different parameter sets (river hydraulic, soil, vegetation)
266 affect model output variables (river discharge, flood extent, river water level, soil
267 moisture, evapotranspiration and terrestrial water storage), multiple model runs were
268 conducted considering four uncalibrated model setups: (1) varying only soil parameters;
269 (2) varying only vegetation parameters; (3) varying only hydraulic parameters; (4)
270 varying all parameters together. One hundred runs were conducted in triplicate to ensure
271 that convergence is not dependent on the initial parameter sets, thus resulting in 300
272 runs for each setup. In this step, no RS-based calibration is performed yet.

273 Parameters were varied considering a uniform distribution, and results were analyzed in
274 terms of mean RMSD (root mean square deviation) of each variable, by comparing each
275 run with a reference one (i.e., the initial run with the initial parameter set as defined in

276 Supplementary Material Table S2). This was performed in order to understand the
277 sources of model uncertainties related to different sets of parameters (e.g., are flood
278 extent estimates sensitive to vegetation parameters, or are ET estimates sensitive to
279 hydraulic parameters?). The dispersion of model outputs was also compared to
280 uncertainty in the observations, as derived from literature.

281 To understand which variables are inter-related in the model, we further analyzed the
282 results of setup “(4) varying all parameters together”. This was done by firstly
283 computing the Kling-Gupta Efficiency metric (KGE; Gupta et al., (2009)) between the
284 perturbed runs and a reference one (i.e., run with the initial parameter set) for each
285 variable, and then calculating the Pearson correlation (r) between KGE values for each
286 pair of variables (e.g., discharge and water level, discharge and flood extent, and so
287 forth). This experiment is relevant to evaluate whether two variables get improved or
288 get worsened together, or whether a variable improvement impacts on the deterioration
289 of another. In other words, this approach allows to evaluate the correlation between the
290 variables.

291

292 **2.6 Model setup**

293

294 The Bare Earth Digital Elevation Model (DEM; O’Loughlin et al., 2016) (Figure 2c)
295 was used for stream network computation and basin discretization with the IPH-
296 HydroTools GIS package (Siqueira et al., 2016). The original DEM resolution is 90 m,
297 and it was resampled to 500 m to facilitate GIS processing. An upstream area threshold
298 of 100 km² was adopted to delineate the drainage network, and unit-catchments were
299 discretized by dividing the stream network into fixed reach length of 10 km, resulting in

300 2957 unit-catchments for the whole basin. Soil type and land cover maps were extracted
301 from the HRU discretization developed by Fan et al. (2015) (Figure 2b): (1) deep and
302 (2) shallow forested areas, (3) deep and (4) shallow agricultural areas, (5) deep and (6)
303 shallow pasture, (7) wetlands, (8) semi-impervious areas, and (9) open water, where
304 “deep soils” refer to soils with high water storage capacity, and “shallow soils” are
305 those with low water storage capacity. In the Purus River Basin, 57.4% of the region is
306 covered by forest with deep soils, 26.9% by forest with shallow soils, and 13.7% by
307 wetlands (i.e., river floodplains). Daily precipitation data were derived from TMPA
308 3B42 (version 7), with spatial resolution of 0.25° x 0.25° (Huffman et al., 2007;
309 available at: <<https://gpm.nasa.gov/data-access/downloads/trmm>>), and were
310 interpolated with the nearest neighbor method for the centroid of each unit-catchment.
311 Long term climate averages for mean surface air temperature, relative humidity,
312 insolation, wind speed and atmospheric pressure were obtained from the Climatic
313 Research Unit database (New et al., 2000; available at:
314 <<http://www.cru.uea.ac.uk/data>>), at a spatial resolution of 10’, and also interpolated
315 with the nearest neighbor method.

316

317 **2.7 Model calibration**

318

319 The MOCOM-UA calibration algorithm (Yapo et al., 1998; Multi-objective global
320 optimization for hydrologic models) was adopted due to its satisfactory performance
321 when coupled with hydrological models (e.g., Collischonn et al., 2008; Maurer et al.,
322 2009; Naz et al., 2014). MOCOM-UA is an evolutionary algorithm, based on SCE-UA
323 (Duan et al., 1992), that simultaneously optimizes a model population with respect to
324 different objective functions. The algorithm converges towards the Pareto optimum,

325 when all points in the population become non-dominated. The model population
 326 consists of randomly distributed points within the parameter search space, and it reflects
 327 the a priori uncertainty of model parameters. Here, the population size was set to 100
 328 individuals. The altered model parameters and their respective ranges are described in
 329 Supplementary Material Table S2. All calibration experiments are repeated three times
 330 (totaling 300 initial runs) with differing initial parameter sets to ensure that convergence
 331 is not dependent on the initial parameter sets. Initial parameters are set as the mean of
 332 their literature-based range (Table S2).

333 Objective functions to be optimized depend on the calibration setup. In the single-
 334 variable calibration, for each variable, three objective functions (*OF*) that summarize
 335 the agreement between simulated and observed (RS) time-series are simultaneously
 336 optimized: Pearson correlation (*r*), ratio of averages (μ_i/μ_{obs}), and ratio of standard
 337 deviations (σ_i/σ_{obs}), which are associated to the individual terms of KGE metric. These
 338 3 objective functions are depicted in Equations 1 to 3, where X denotes the assessed
 339 variables (Q, h, A, TWS, ET or W).

$$340 \quad OF_1 = \left(\frac{\mu_i}{\mu_{obs}} \right)_X (1); OF_2 = \left(\frac{\sigma_i}{\sigma_{obs}} \right)_X (2); OF_3 = r_X (3)$$

341 For the multi-variable calibration, the objective functions are the KGE of each variable
 342 considered: firstly, five objective functions were considered (KGE of all variables
 343 except discharge), as depicted in Equations 4 to 8.

$$344 \quad OF_1 = KGE_h (4); OF_2 = KGE_A (5); OF_3 = KGE_{TWS} (6); OF_4 = KGE_{ET} (7); OF_5 = KGE_W (8)$$

345 Secondly, two objective functions were adopted and simultaneously calibrated (KGE of
 346 selected variables 1 (x) and 2 (y)), as depicted in Equations 9 and 10.

$$347 \quad OF_1 = KGE_x (9); OF_2 = KGE_y (10)$$

348 Results are expressed in terms of a Skill Score (S) (Equation 11; Zajac et al., 2017), in
349 order to evaluate the improvement (or deterioration) in the representation of a variable
350 when the model is calibrated with a given variable, compared to the uncalibrated setup.

351

$$352 \quad S = \frac{KGE_{calibrated} - KGE_{initial}}{1 - KGE_{initial}} \quad (11)$$

353

354 $KGE_{calibrated}$ is the mean KGE resulting from running the model with the
355 calibrated parameters. $KGE_{initial}$ is the mean KGE resulting from running the model with
356 the a priori parameter sets (i.e., randomly selected parameters within an a priori range of
357 parameter values).

358

359 **2.8 Calibration/Evaluation Data**

360 In the next paragraphs we introduce the data used for model calibration and evaluation,
361 as well as how MGB outputs were evaluated in comparison to them.

362 *-In-situ discharge measurements* were obtained from the Brazilian Water Agency
363 Hidroweb database (available at:
364 <<http://www.snirh.gov.br/hidroweb/publico/apresentacao.jsf>>), at the gauge
365 “Canutama” (code: 13880000; location: S ° 32' 20.04"; W 64° 23' 8.88"; drainage area:
366 236,000 km², period of data availability: 1973 to 2016). Uncertainty in discharge
367 observations can be estimated as ranging from 6.2% to 42.8% at the 95% confidence
368 level, with an average of 25.6% (Di Baldassarre & Montanari, 2009). Discharge was
369 evaluated on a daily basis.

370 - *Remotely sensed water level data* were obtained from Jason-2 mission, which presents
371 an orbit cycle of approximately 10 days, and tracks separated by approximately 300 km
372 at the equator (Lambin et al., 2010). It presents an accuracy of approximately 0.28 m
373 (Jarihani et al., 2013), and data are available since 2008. The virtual station presented in
374 Figure 1 corresponds to Track number 165. Processed data for this study were
375 downloaded from the Hydroweb/Theia database (available at: [http://hydroweb.theia-](http://hydroweb.theia-land.fr)
376 [land.fr](http://hydroweb.theia-land.fr)). Water level was computed in MGB at the unit-catchment associated to the
377 altimetry virtual station, being an advantage of using the hydrodynamic scheme for
378 flood routing instead of the Muskingum simplification. Simulated and RS water level
379 data were compared every 10 days in terms of anomaly (values subtracted from long
380 term average).

381 - *Satellite flood extent data* were derived from ALOS-PALSAR imagery, which
382 presents a ground resolution of 100 m (Rosenqvist et al., 2007). Images were
383 downloaded from Alaska Satellite Facility (available at: <https://www.asf.alaska.edu/>)
384 in processing level 1.5, which already presents geometric and radiometric corrections. A
385 3 x 3 median filter was used to remove speckle noise (Lee et al., 2014). Images were
386 classified into water (backscattering coefficient less than -14 dB), non-flooded forest
387 (between -14 dB and -6.5 dB), and flooded forest (higher than -6.5 dB) classes,
388 according to Hess et al. (2003) and Lee et al. (2014). The uncertainty of flood extent
389 estimates was estimated based on the RMSE between the resulting classification of this
390 study, and the dual-season mapping developed by Hess et al. (2003). Simulated and RS
391 flood extent data were compared for the pink area depicted in Figure 1, in order to avoid
392 spurious flood extent data in regions that are known to be not subject to flooding.
393 ALOS-PALSAR presents a recurrence cycle of 46 days (from 2006 to 2011), and flood
394 extent data were available and compared to MGB for 21 dates.

395 - *Satellite-based terrestrial water storage (TWS) anomalies* were extracted from
396 GRACE mission, launched in March 2002. GRACE provides monthly TWS estimates
397 based on anomalies in gravitational potential, at a resolution of 300-400 km, with a
398 uniform accuracy of 2 cm over the land and ocean regions (Tapley et al., 2004). TWS
399 anomalies were retrieved from three processing centers - GFZ (Geoforschungs Zentrum
400 Potsdam, Germany), CSR (Center for Space Research at University of Texas, USA),
401 and JPL (Jet Propulsion Laboratory, USA), available at <<https://grace.jpl.nasa.gov/>>,
402 and then the mean value based on the three products was averaged for the whole basin.
403 In MGB, TWS values were computed as the sum of water storage of all hydrological
404 compartments: river, floodplains, soil, groundwater and vegetation canopy. Simulated
405 and RS-based TWS were compared in terms of anomaly (values subtracted from long
406 term average) at a monthly time-scale.

407 - *Satellite-based evapotranspiration* estimates were retrieved from the MOD16 product,
408 derived by an algorithm presented by Mu et al. (2011) based on the Penman-Monteith
409 equation. The dataset covers the period 2000-2010 with a spatial resolution of 1 km for
410 global vegetated land areas. Because of that, even though MGB evapotranspiration is
411 calculated for flooded areas (open water evaporation in main channel and floodplains)
412 and vegetation for water balance purposes, only the vegetation-ET output was compared
413 to MOD16. MOD16 products are provided in 8-days, monthly and annual intervals.
414 Monthly intervals were used here and averaged for the whole basin. Accuracy of
415 MOD16 along the Amazon basin is estimated as 0.76 mm/day (Gomis-Cebolla et al.,
416 2019). MOD16 data is available at: <
417 <https://www.ntsg.umt.edu/project/modis/mod16.php>>. In MGB, evapotranspiration is
418 computed via Penman-Monteith equation, based on the climate input variables.

419 - *Satellite-based soil moisture* is derived from the SMOS mission (Kerr et al., 2001),
420 processed by the Centre Aval de Traitement des Données SMOS (CATDS), and
421 downloaded in processing level 4, which combines lower level products with data from
422 other sensors and modeling/data assimilation techniques. The daily L4 root zone soil
423 moisture product at 0-1 m soil depth (Al Bitar et al., 2013) were used (available at:
424 <[https://www.catds.fr/Products/Available-products-from-CEC-SM/L4-Land-research-](https://www.catds.fr/Products/Available-products-from-CEC-SM/L4-Land-research-products)
425 [products](https://www.catds.fr/Products/Available-products-from-CEC-SM/L4-Land-research-products)>), and data from ascending and descending orbits were averaged for the whole
426 basin. In MGB, soil moisture as a saturation degree was computed as the water in the
427 soil compartment divided by the maximum water capacity of the soil (W_m parameter).
428 Since MGB estimates saturation degree values for a soil bucket reservoir, SMOS values
429 were rescaled for the range 0 - 100% according to the Min/Max Correction method
430 described by Tarpanelli et al. (2013) and applied by some studies (e.g., Rajib et al.,
431 2016; Silvestro et al., 2015), and them compared to MGB on a daily time-scale as an
432 average for the whole basin.

433

434 **3 Results and discussion**

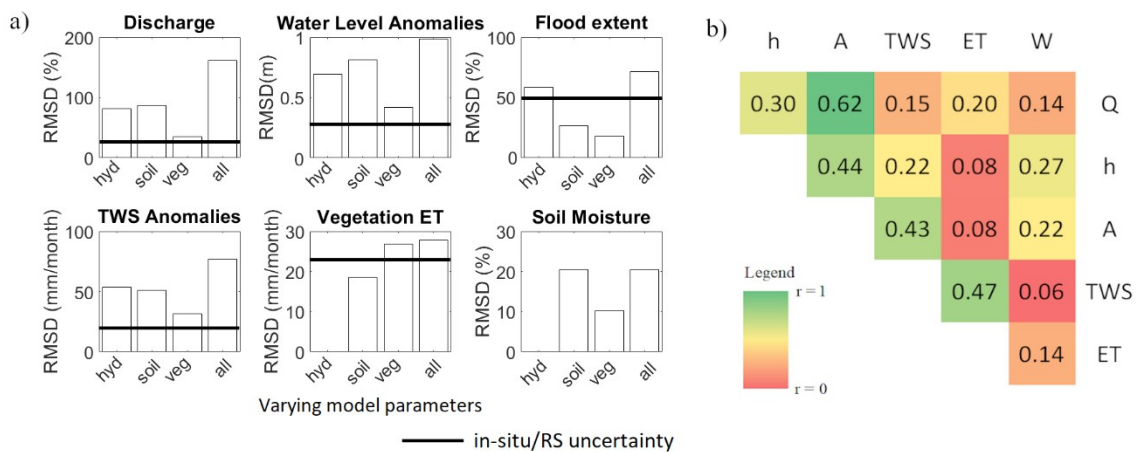
435 Results are structured as follows. Firstly, the sensitivity analysis is presented with
436 discussions on model uncertainties (Section 3.1). Then, results for model calibration are
437 presented, with discussions on how RS-based model calibration can improve discharge
438 and the water cycle representation as a whole (Section 3.2).

439

440 **3.1 Sensitivity analysis**

441 A sensitivity analysis was carried out to understand how different parameter types (river
 442 hydraulic, soil, vegetation, and all together) affect the variation of different hydrological
 443 processes in MGB (Figure 3a). This was performed by analyzing the dispersion of six
 444 output variables (discharge, water level, flood extent, TWS anomalies, vegetation ET,
 445 and soil moisture). These results are also compared with an estimate of the uncertainties
 446 of observations (values provided in section 2.8 *Calibration/Evaluation Data*), and are
 447 discussed in the subsequent sections.

448



449

450 **Figure 3. a)** Sensitivity analysis of different model output variables to varying sets of
 451 parameters (hyd=hydraulics, soil, veg=vegetation, and all together). The a priori dispersion of
 452 the model parameters, for each output variable, is compared to the reported uncertainty for the
 453 in-situ / RS product estimates, previously described in the Cal/Eval data section (no uncertainty

454 estimation is provided for the soil moisture root zone product given absence of this estimate for
455 the Amazon region). **b)** Correlation matrix (Pearson coefficient) between performance metrics
456 (KGE) for the six analyzed variables, by varying all parameters together. KGE values are
457 computed by comparing multiple runs with the reference simulation (i.e., the initial run with
458 the initial parameter set as defined in Supplementary Material Table S2). Q = discharge,
459 h = water level, A = flood extent, TWS = total water storage anomalies, ET = vegetation
460 evapotranspiration, W = soil moisture.

461

462 **3.1.1 How do varying model outputs relate to uncertainty in the observations?**

463 Some variables present in-situ/RS observations that have uncertainties significantly
464 lower than the overall dispersion of the model, e.g., 25 % for discharge observations,
465 while model overall parameter dispersion is ~160%. This pattern is also found for water
466 level and TWS estimates, and implies that these observations might be useful to
467 constrain the model. Nonetheless, uncertainties in RS products of flood extent (~50%)
468 and vegetation ET (~23%) are in the same order of magnitude of model overall
469 parameter dispersion, which might hamper their contribution for model calibration, due
470 to their high uncertainties.

471

472 **3.1.2 Which sets of parameters are related to which variables?**

473 The overall model dispersions are related to different sets of parameters: discharge,
474 water level, and TWS are more strongly related to hydraulics and soil parameters, and to
475 a lesser extent to vegetation parameters. Flood extent estimates are strongly related to
476 hydraulic parameters, and less to soil and vegetation. As expected, soil moisture and
477 vegetation ET estimates relate to vertical water balance processes, being insensitive to
478 hydraulic parameters. Soil moisture (W) is more sensitive to soil parameters, while

479 vegetation ET is more sensitive to vegetation parameters. These results are very useful
480 to understand the RS-based calibration experiments addressed in section 3.2. For
481 instance, if model calibration with ET or W is achieved through optimization of
482 hydraulic parameters, it would highlight that the model would have “gotten the right
483 results for the wrong reasons”. The same would occur if flood extent calibration
484 targeted soil or vegetation parameters.

485

486 **3.1.3 Which variables are inter-related?**

487 By varying all parameters together, there is a high correlation (greater or equal to 0.4)
488 between the performance of discharge and flood extent, water level and flood extent,
489 flood extent and TWS, and ET and TWS (Figure 3b). High correlations between
490 discharge, water level and flood extent are expected because of their strong association
491 through river transport processes. However, correlation between discharge and water
492 level is not too high (0.30), and this is probably due to high uncertainties in hydraulic
493 parameters, and to the large distance separating the water level virtual station and the
494 streamflow gauge. Furthermore, high correlations between TWS and flood extent might
495 be related to surface water storage dynamics which are especially relevant in regions
496 with floodplains.

497 In general, a high correlation between variables in Figure 3b should be reflected in
498 positive results when calibrating with a given variable and evaluating with the other
499 highly correlated variable (single-variable calibration). This may also indicate that
500 observations of these variables are redundant if used simultaneously in a multi-
501 calibration framework. However, high correlations in Figure 3b followed by
502 deterioration after the single-variable calibration process might indicate structural errors
503 in the model, or in the observations. We stress however that this study did not attempt to

504 quantify structural errors. Conversely, low correlations in Figure 3b, followed by
505 improvement in performances with the calibration with multiple variables, might
506 indicate complementarity between variables.

507

508 **3.2 Model calibration**

509

510 **3.2.1 How RS-based model calibration improves discharge estimates?**

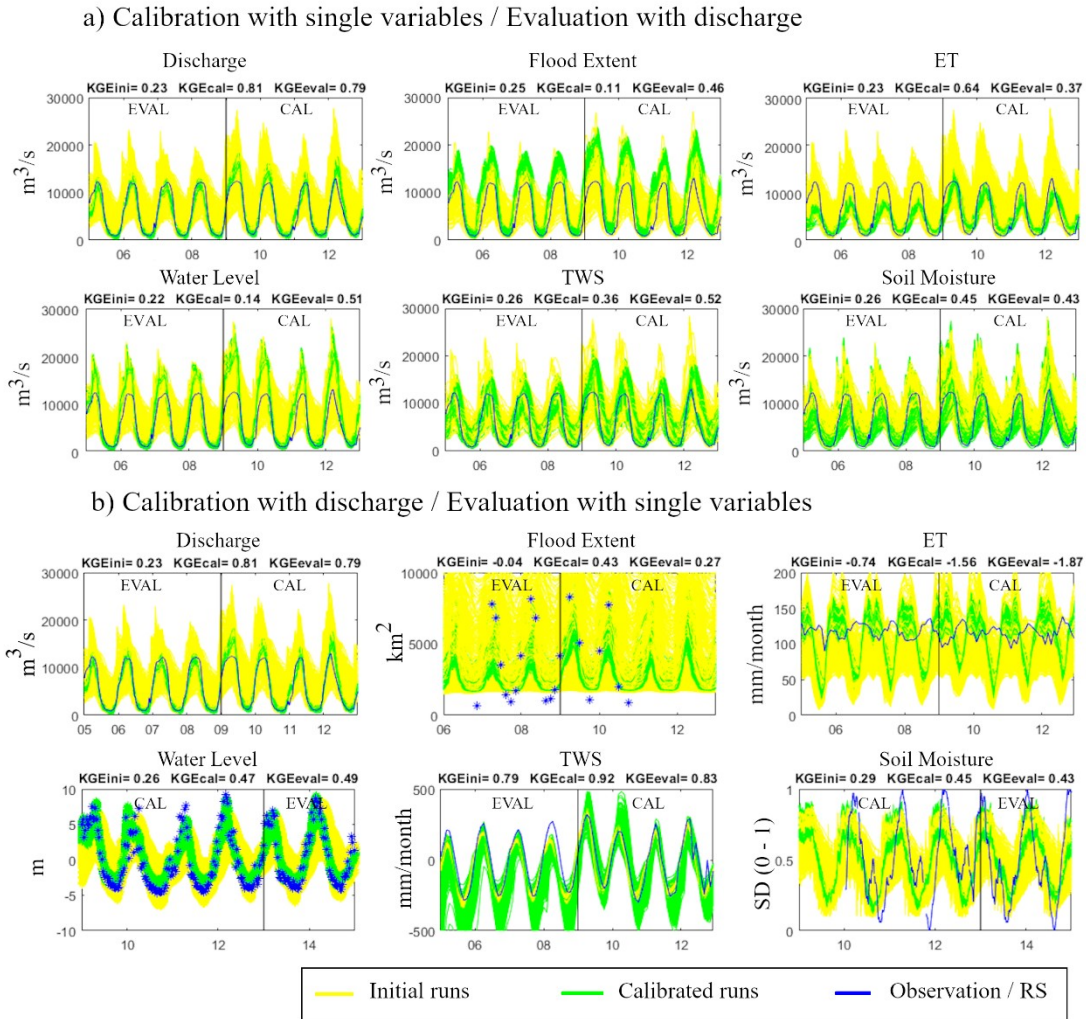
511 For the evaluation time period (2006–2008 for discharge, flood extent, TWS, ET and
512 2013–2014 for water level and soil moisture), calibration with all RS products led to
513 improvements in discharge estimates (Figure 4a). For the calibration time period (2009-
514 2012), TWS, ET and soil moisture RS products also led to improvements in discharge
515 estimates, while water level and flood extent led to discharge overestimation in wet
516 periods (Figure 4a). This could be due to high uncertainties in the observations (Figure
517 3a), but if this was the case, it would also be reflected in a poor performance for water
518 level and flood extent when discharge is the target variable for calibration (Figure 4b),
519 which does not occur. Therefore, calibration with discharge leads to reasonable
520 parameter sets for the performance of discharge itself, and also water level and flood
521 extent. However, it does not lead to the best hydraulic arrangement, which might be
522 achieved more successfully when calibrating with water level or flood extent.

523 Nonetheless, both water level and flood extent observations are representative of a
524 specific location in the basin (Figure 2), and calibration with these variables might lead
525 to the best parameter arrangement for these locations, but not for the whole watershed.
526 A more spatially-consistent use of these observations should improve their usability to
527 constrain models and improve discharge estimates, such as the studies of Kittel et al.

528 (2018), that used radar altimetry measurements at 12 locations in the basin, Schneider et
529 al. (2017), that used data from 13 virtual stations, or Liu et al. (2015), that used water
530 level measurements at four virtual stations, and flood extent for stream segments at
531 different locations in the basin.

532 RS variables as TWS, ET, and soil moisture were able to improve discharge estimates
533 by $S = 13.7\%$ ($KGE_{cal}=0.36$), $S = 52.9\%$ ($KGE_{cal}=0.64$), and $S = 27.0\%$ ($KGE_{cal}=0.45$)
534 (Figure 5-I, calibration period) or $S = 27.4\%$ ($KGE_{eval}=0.52$), $S = 6.1\%$ ($KGE_{eval}=0.37$),
535 $S = 12.3\%$ ($KGE_{eval}=0.43$) (Figure 5-II, evaluation period), which is especially relevant
536 in the context of the Prediction in Ungauged Basins initiative (Hrachowitz et al., 2013;
537 Sivapalan et al., 2003). These results agree with previous studies, such as López et al.
538 (2017) that found good performances in discharge estimates by model calibration with
539 GLEAM ET and ESA CCI soil moisture, or Nijzink et al. (2018), that found
540 improvements in discharge by using soil moisture products (AMSR-E, ASCAT) and
541 TWS from GRACE.

542 The multi-variable calibration experiment considering all variables except discharge
543 (Figure 5b) resulted in a Skill Score of $S = 17.4\%$ ($KGE_{eval}=0.45$) for discharge in the
544 evaluation period. This is relevant for estimating discharge in poorly gauged basins.
545 Nonetheless, for the calibration period, Skill Score had a low value ($S = 1.7\%$,
546 $KGE_{cal}=0.25$), reflecting some limitations when retrieving discharges, probably because
547 of potential trade-offs between variables (Koppa et al., 2019). RS uncertainties can be
548 reduced in model calibration, for instance by using bias-insensitive metrics (e.g.,
549 Demirel et al., 2018; Zink et al., 2018; Dembele et al., 2020), or explicitly including
550 them into the objective functions (Aires, 2014; Croke, 2009; Foglia et al., 2009; Peña-
551 Arancibia et al., 2015).

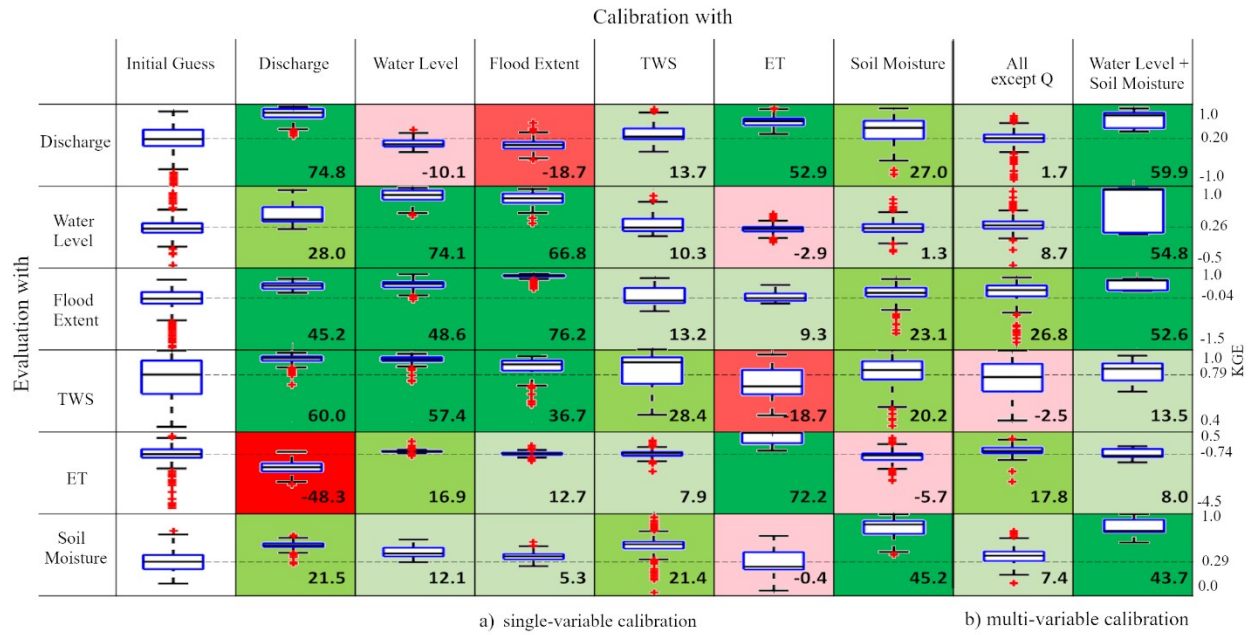


552

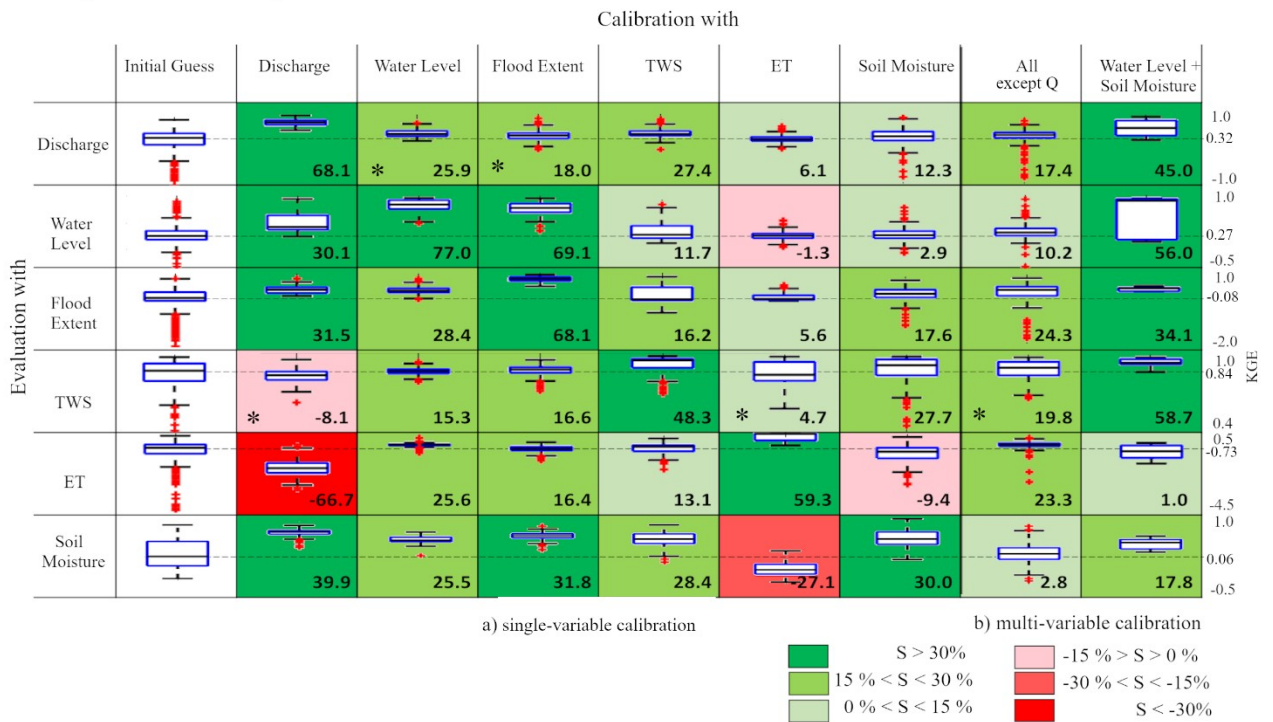
553 **Figure 4.** (a) Daily time series of discharge, when calibrating the model with six different
 554 variables. (b) Time series of the six variables when calibrating the model with discharge
 555 observations only (discharge, water level, flood extent and soil moisture are at a daily time step,
 556 while TWS and ET are at a monthly time step). *KGEini* is the mean KGE of initial runs,
 557 *KGEcal* is the mean KGE of calibrated runs, evaluated for the same period of calibration,
 558 *KGEeval* is the mean KGE of calibrated runs, evaluated for a different period than calibration.
 559 Time series for all variables by calibrating the model with all setups is presented in
 560 Supplementary Material (Figure S1).

561

I) Evaluation for the period of calibration



II) Evaluation for a period different than calibration



562

563 **Figure 5.** Boxplots of mean KGE for the evaluation of multiple variables with different
 564 calibration strategies. (I) Evaluation for the period of calibration (2009 – 2012); (II) Evaluation
 565 for a different period than calibration (2006 – 2008 for Q, A, TWS, ET; 2013 – 2014 for h and
 566 W). “Initial guess” refers to model runs with the a priori parameter sets. (a) Single-variable
 567 (discharge, water level, flood extent, TWS, vegetation ET, soil moisture) and (b) multi-variable

568 calibration (all except discharge, water level + soil moisture). The spread of the values in the
569 boxplots stems from 300 model runs (100 for each of three calibration experiments). Numbers
570 next to the boxplots represent Skill Score (%). Colors refer to classes of skill score. Please note
571 that the KGE scales are different for each variable. Asterisks refer to cases when the evaluation
572 period resulted in a different performance than the calibration period (i.e., positive Skill Score in
573 calibration followed by negative Skill Score in evaluation, or vice-versa). Please note that Skill
574 Score values are computed based on mean values, while the boxplots depict median values.

575

576 **3.2.2 How does RS-based model calibration improve the water cycle** 577 **representation?**

578 When performing a single-variable calibration, the performance of the variable itself
579 always improves, which is evidenced by the positive values in the main diagonal
580 (Figure 5-I-a, for calibration period, and Figure 5-II-a, for evaluation period).
581 Calibration with water level was also able to improve estimates of flood extent, TWS,
582 ET and soil moisture (cal period), and all variables (eval period). Calibration with flood
583 extent improved water level, TWS, ET and soil moisture. Calibration with TWS
584 improved all variables. Calibration with ET was able to improve discharge and flood
585 extent. Calibration with soil moisture improved all variables but ET. Results for
586 calibration and evaluation periods agree (i.e., improvement (positive Skill Score) or
587 deterioration (negative Skill Score) for both cal and eval) in 43 out of the 48 cases
588 (89.6%). In the five remaining cases (10.4%), results between calibration and evaluation
589 periods differ: three of them are in the evaluation with TWS, and two of them are in the
590 discharge evaluation (calibration with water level and flood extent).

591 In the best modeling scenario, calibration with any variable should improve the
592 performance of all other variables. However, we have identified that this did not happen

593 in our experiments. This can be due to uncertainties in model structure, in
594 parameterization, in the observations, or the integration techniques in model calibration
595 (Dembele et al., 2020). Previous studies have also found significant advantages in using
596 RS-based model calibration to identify structural model issues (e.g., Werth et al., 2009;
597 Willem Vervoort et al., 2014; Winsemius et al., 2008), detect uncertainties in input data
598 (e.g., Milzow et al., 2011), identify deficiencies in model parameterization (e.g., Franks
599 et al., 1998; Koppa et al., 2019), or increase model reliability (e.g., Koch et al., 2018;
600 Manfreda et al., 2018).

601 According to Figure 4b and Supplementary Material (Figure S1), calibration with
602 discharge improved estimates of almost all variables. However, calibration with
603 discharge deteriorated the performance for vegetation ET time series. Vegetation ET
604 estimated by MOD16 varies at maximum 30mm/month. MGB calibration with
605 discharge led to ET variations of 100 mm/month, reaching around 30 mm/month in the
606 driest periods, while MOD16 estimates are limited to a minimum of 100 mm/month in
607 these periods (time series in Figure 4b). However, one can notice that not even the
608 seasonality between MGB and MOD16 time series agree. This could be due to
609 relatively high uncertainties in vegetation ET estimates from MOD16 for the Amazon
610 basin (around 23 mm/month, according to Gomis-Cebolla et al., 2019). Nonetheless, it
611 could also be related to model structural and/or parameter deficiencies, in which case
612 the model might be “right for the wrong reasons”. In order to identify the source of this
613 ET inconsistency, we have compared MOD16 and MGB results to in-situ measurements
614 of ET in Purus River Basin, provided by Gomis-Cebolla et al. (2019) and Maeda et al.
615 (2017). We found a much stronger agreement both in seasonality and in amplitude of in-
616 situ observations with MOD16 observations than with MGB model output. Hasler &
617 Avissar (2007) and Pan et al (2020) have already warned about the overestimation of

618 dry season water stress in hydrological models, probably related to the
619 misrepresentation of soil water availability for plants. This was also found by Maeda et
620 al. (2017), which highlighted that ET was not water-limited because of the plants'
621 access to deep soil water, which has also been previously documented by Nepstad et al.
622 (1994). They found that, in the Southern Amazon ecotone, deep root water intake plays
623 a key role in maintaining ecosystem productivity during dry season. MGB model is
624 probably misrepresenting these processes, which would remain unknown if it were only
625 compared to discharge time series.

626 Even though the calibration with discharge observations was not able to accurately
627 estimate ET, calibration with the remaining variables (except for soil moisture) was able
628 to improve ET estimates. For instance, in Figure 3b, ET and water level presented low
629 correlation ($r = 0.08$), but calibration with water level improved ET estimates by $S =$
630 16.9% (cal period) and $S = 25.6\%$ (eval period). However, in Figure 3b, ET and TWS
631 presented high correlation ($r=0.47$), but calibration with TWS improved ET estimates
632 by only $S = 7.9\%$ (cal period) and $S = 13.1\%$ (eval period).

633 In general, calibration with TWS did not present much influence on any of the variables.
634 In spite of some improvements, skill scores were usually low. Consistently, TWS
635 estimates got relatively easily improved by calibration with any variable (except for ET,
636 for cal period; or discharge, for eval period). These results for TWS contrast with
637 previous work from Lo et al. (2010), Nijzink et al. (2018), Rakovec et al. (2016),
638 Schumacher et al. (2018), and Werth & Güntner (2010), which highlighted the value of
639 GRACE data when incorporated into hydrological modeling. This can be due to the
640 high seasonality of Purus River Basin, in which TWS does not aggregate much
641 information, biasing the calibration with high correlation values. Even for the initial
642 guess (uncalibrated) setup TWS performances were already very good: KGE values

643 were around 0.8, while for all other variables, except for ET (for which KGE values
644 were negative), KGE values were around 0.3 for the uncalibrated setup.

645 Flood extent and water level performances were improved by calibration with
646 discharge, water level and flood extent, but it did not affect much ET (which actually
647 was degraded with discharge calibration) and soil moisture. This is probably due to the
648 relationship between water level and flood extent with river transport processes (e.g.,
649 flood routing and floodplain storage), while ET and soil moisture are more related to
650 vertical hydrological processes (e.g., soil water balance). This highlights the
651 complementarity between variables that relate to different processes.

652 Calibration with soil moisture improves performances of all variables (water level to a
653 lesser extent), except for ET. Consistently, calibration with all variables (except ET) are
654 able to improve soil moisture to some extent.

655

656 **3.2.3 What is the added value of complementary RS observations?**

657 By calibrating with all variables together except Q (Figure 5b), we found improvements
658 for almost all variables, with the most significant improvements for flood extent ($S =$
659 25% for cal and eval periods) and ET ($S = 20\%$ for cal and eval periods). For discharge,
660 performance for the evaluation period was improved ($S = 17.4\%$), which is important
661 for estimating discharge in poorly gauged basins. However, for the calibration period,
662 Skill Score for discharge performance was $S = 1.7\%$, which might reflect some
663 limitations in retrieving discharge based on the calibration of the RS-derived variables,
664 as discussed previously.

665 Therefore, we chose a specific arrangement of two complementary variables in order to
666 check if this calibration setup might lead to better retrievals for discharge and the other

667 variables. The chosen variables were soil moisture and water level, because of their
668 complementarity. Based on the Skill Score values in Figure 5-I, calibration with water
669 level only improves all variables but discharge (and soil moisture to a lesser extent),
670 while calibration with soil moisture only improves all variables, but ET (and water level
671 to a lesser extent).

672 The calibration arrangement of water level and soil moisture led to improvements not
673 only to soil moisture and water level themselves, but also to all other variables (ET to a
674 lesser extent). For instance, flood extent was improved by $S = 52.6\%$ and $S = 34.1\%$
675 (cal and eval period, respectively). Discharge was improved by $S = 59.9\%$, with a
676 resulting mean KGE = 0.70 for the calibration period ($S = 45.0\%$ and mean KGE = 0.35
677 for evaluation period). These results agree with previous works that found an
678 improvement in model performances by multi-variable calibration of soil moisture and
679 evapotranspiration (e.g., Koppa et al., 2019; López et al., 2017), discharge and
680 evapotranspiration (e.g., Herman et al., 2018; Pan et al., 2018; Poméon et al., 2018),
681 discharge and soil moisture (e.g., Li et al., 2018; Rajib et al., 2016), discharge and TWS
682 (e.g., Rakovec et al., 2016; Schumacher et al., 2018; Werth & Güntner, 2010), and
683 discharge and water level (e.g., Kittel et al., 2018; Schneider et al., 2017; W. Sun et al.,
684 2012). However, it is difficult to compare this study to previous works, because most of
685 them used discharge observations as constraints. In this study, we avoided the use of
686 discharge observations for multi-variable calibration, in order to analyze the
687 applicability of the RS-based calibration method for poorly-gauged regions.

688 Calibration with water level and soil moisture did not present much influence on ET
689 performance, because of the specificities regarding ET in this watershed, i.e., given that
690 the model setup does not represent deep root water intake during dry season, as
691 discussed previously.

692 By comparing the two frameworks for multi-variable calibration (all except Q versus
693 h+W calibration), we found that calibration with all variables except Q is useful to some
694 extent, but consistently selecting complementary variables for model calibration
695 resulted in best overall performance.

696

697 **3.3 Are we getting the right results for the right sets of parameters?**

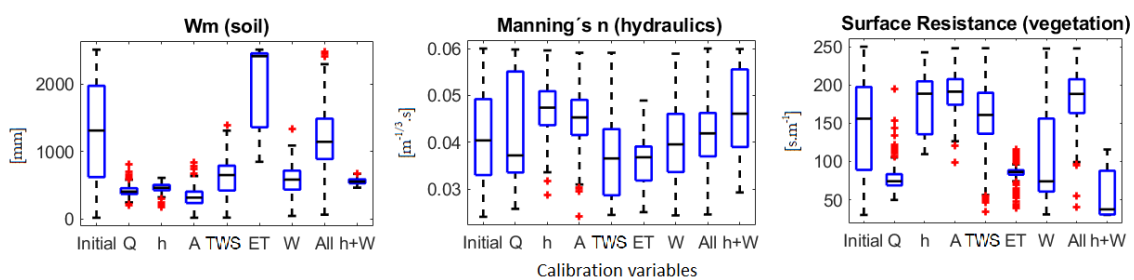
698 When analyzing the dispersions of parameters before and after calibration with each
699 variable (Figure 6 for a few selected parameters, Supplementary Material Figure S2 for
700 all calibrated parameters), it can be observed that the range of parameters varies largely
701 depending on the calibration variable. For instance, W_m is a soil conceptual parameter
702 related to maximum water storage in the soil. In the calibration based on single
703 variables (except ET) it converged to low values (300 mm), while in the calibration with
704 ET it reached high values (2000 mm). This probably occurred in order to compensate,
705 by overparameterization, a structural error in the model, i.e., the model inability to
706 represent deep root water uptake in dry season. These trade-offs between model
707 parameters during calibration has also been reported and discussed by Koppa et al.
708 (2019).

709 The surface resistance parameter also resulted in a wide range of values depending on
710 the calibration target variable. When calibrated with water level, flood extent, or ‘all
711 except Q’ experiments, it reached median values higher than 150 s/m, but calibration
712 with h+W led to median values lower than 50 s/m. Surface resistance is a vegetation
713 parameter directly related to ET dynamics, so it is important to note that calibration with
714 ET was able to reduce the dispersion of this parameter, reaching a median value of
715 about 80 s/m (similar to calibration with Q and W).

716 Another interesting result relates to channel Manning's coefficient, which presented
 717 different values for each calibration experiment. This agrees with previous findings
 718 about Manning parameter being often used as an effective parameter that compensates
 719 for neglected hydrodynamic processes as localized channel head losses, poor cross
 720 section representation, or non-represented 2D processes (Neal et al 2015).

721 Many previous studies have highlighted the use of multi-variable calibration to narrow
 722 parameters' search space (Nijzink et al., 2018; W. Sun et al., 2018), but this was not
 723 observed in our results. Based on the limited multi-variable calibration experiments
 724 performed here ('all except Q' and h+W), no narrowing in parameters' search space
 725 was found. For most parameters (except for Wm), calibration with 'all except Q' and
 726 h+W resulted in a wide range of values. This can be due to differing convergence sets of
 727 parameters between each of the triplicate runs. A more robust experiment comparing
 728 more multi-variable calibration strategies (e.g., Q + different R-based variables) might
 729 provide better understanding on this topic.

730



731

732 **Figure 6.** Boxplots of dispersion of three model parameters before (Initial) and after the single-
 733 variable calibration (Q – discharge; h – water level; A – flood extent; TWS – total water
 734 storage anomalies; ET - vegetation ET; W – soil moisture), and multi-variable calibration (All
 735 – variables except discharge; h+W – water level and soil moisture). The spread of the values in
 736 the boxplots stems from 300 model runs (100 for each calibration experiment). Description of

737 parameters is presented in Supplementary Material Table S2. A complete figure with boxplots
738 for all parameters is presented in Supplementary Material Figure S2.

739

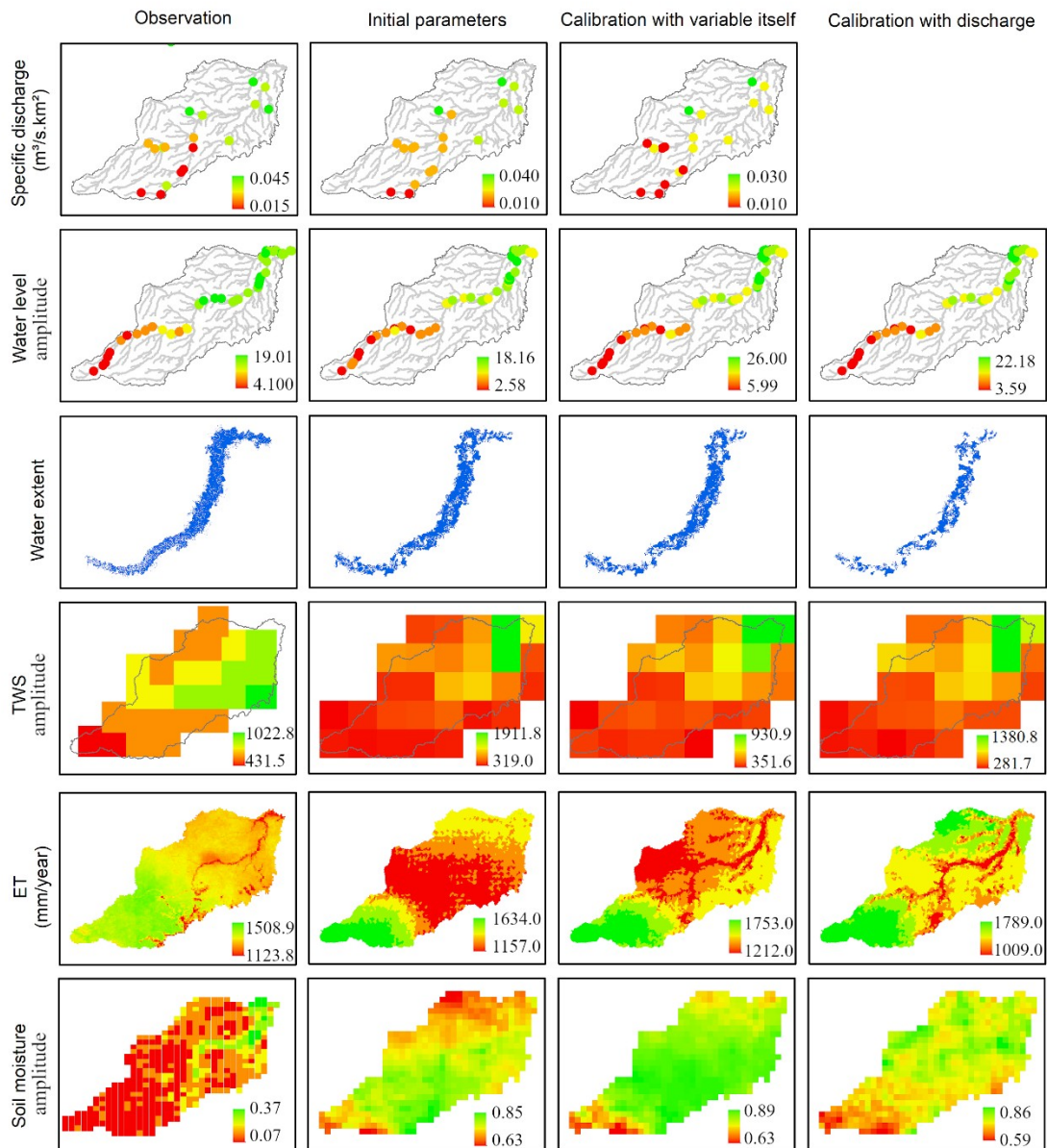
740 **3.4 Spatial Evaluation**

741 For model calibration, we used one streamflow gauge for discharge, one virtual station
742 for water level, and averaged RS data for the whole basin for TWS, ET and soil
743 moisture. However, many recent studies investigated the potential for using RS spatially
744 distributed information in model calibration, for instance with bias-insensitive metrics
745 (Demirel et al., 2018; Zink et al., 2018; Dembele et al., 2020). Here we further analyze
746 how the lumped calibration affected the simulated spatial patterns (Figure 7; Figure S3
747 in Supplementary Material).

748 For discharge, water level, flood extent and TWS, spatial patterns are well reproduced
749 even when running the model with the initial parameter set, because the spatial patterns
750 of these variables are determined by intrinsic characteristics of the basin. Nonetheless,
751 for ET, the spatial patterns are completely different between the initial parameter set and
752 the calibrated setup. In this case, the calibration with spatially aggregated ET was able
753 to recover the spatial representation of MOD16. A similar result was found for soil
754 moisture spatial representation by Demirel et al. (2019), that calibrated a model with
755 spatially aggregated soil moisture and TWS data.

756 In summary, these results highlight the overall model capability to retrieve the ET
757 spatial pattern even by using a lumped calibration approach. However, for other
758 variables, the spatial pattern was not considerably affected by the differing model
759 calibration strategies.

760



761

762 **Figure 7.** Spatial distribution of variables. Columns: RS observation, model run with the
 763 initial parameter set, model run with the best parameter set (calibrated for each
 764 variable), model run with the best parameter set (when calibrated with discharge).

765 Complete figure is presented in Figure S3 (Supplementary Material).

766

767

768

769 4 Conclusion

770 We calibrated and evaluated a hydrologic-hydrodynamic model with five different RS-
771 based observations of the water cycle: water levels (Jason-2), flood extent (ALOS-
772 PALSAR), TWS (GRACE), vegetation ET (MOD16), and soil moisture (SMOS), for a
773 study basin in a tropical region with floodplains (Purus River Basin in the Amazon), and
774 analyzed the redundancy and complementarity between different variables and
775 processes.

776 Results showed that calibration with current RS observations was able to improve
777 discharge estimates. For instance, in the uncalibrated setup (a priori parameter sets),
778 average performances for discharge were around $KGE = 0.30$. By calibrating the model
779 with ET from MOD16 (and evaluating for the same time period), discharge average
780 performance was improved to $KGE = 0.64$, representing a Skill Score of $S = 52.9\%$.
781 Also in the calibration period, a joint scheme of calibration with water level + soil
782 moisture led to discharge improvements of $S = 59.9\%$. When evaluating for a different
783 time period, discharge performance was improved by calibration with water level, TWS
784 and a joint scheme of all RS-variables ($S = 25.9\%$, $S = 27.9\%$ and $S = 17.4\%$,
785 respectively). We conclude that RS observations are useful to predict discharge
786 estimates. However, the utility of each RS variable might depend on the study area
787 characteristics and the time period considered.

788 Our results also showed that RS-based calibration led to an overall improvement of the
789 water cycle representation. For instance, calibration with water level was able to
790 improve estimates of water level itself, but also flood extent, TWS and ET; calibration
791 with soil moisture was able to improve estimates of soil moisture itself, but also
792 discharge, flood extent and TWS.

793 Moreover, calibration with multiple RS variables was able to highlight deficiencies that
794 might be related to model structure, parameterization, observations, and data integration
795 techniques in model calibration. In the context of model structure, for instance,
796 calibration with ET highlighted the model inability to represent the root water intake in
797 dry season in this region, thus compensating it by misrepresenting other variables. In the
798 context of model parameterization, for instance, we found a wide range of different
799 parameters by varying the calibration target variable.

800 Besides individual calibration with each RS variable, we conducted two multi-variable
801 calibration experiments: calibration with all variables except discharge, and calibration
802 with water level and soil moisture. Calibration with all variables was useful to some
803 extent, but appropriately selecting complementary variables for model calibration may
804 result in a better overall performance. Even though we used a lumped calibration
805 approach, results highlighted the overall model capability to retrieve ET spatial pattern,
806 but not for TWS and soil moisture.

807 The main conclusions presented here are of great interest for the hydrological
808 community, and agree with previous works in that RS-based calibration is useful to
809 improve the water cycle representation in hydrological models. To further investigate
810 the potentiality of RS data, future developments should test the methodology presented
811 here for multiple basins at contrasting hydro-climatic regions. Here, we assessed an
812 Amazonian Equatorial basin, with particular climate and land cover characteristics and
813 an overall spatial homogeneity of rainfall-runoff processes. Other basins with different
814 hydroclimatic regimes could be also assessed, e.g., in arid basins subject to long dry
815 periods, more erratic precipitation patterns, and different runoff generation mechanisms
816 than the Amazon, which require different model structures.

817 Finally, here we used one state-of-the-art RS product for each variable, but future
818 developments should explore other missions like SWOT for surface water observation
819 (Biancamaria et al., 2016), as well as considering different products for representing
820 each variable (e.g., ET could be estimated by GLEAM, MODIS, SSEBop, SEBS,
821 ALEXI, METRIC, etc., besides MOD16).

822

823 **Acknowledgements**

824 This study was financed in part by the Coordenação de Aperfeiçoamento de Pessoal de
825 Nível Superior - Brasil (CAPES) - Finance Code 001, and the Conselho Nacional de
826 Desenvolvimento Científico e Tecnológico (CNPq) – Grant Number 41161/2017-5. It
827 was conducted in the context of the SWOT-MOD science team project from SWOT
828 satellite mission. We would also like to thank colleagues from the Large Scale
829 Hydrology Group (HGE/IPH) for general discussions about this study. Data presented
830 in this study are available at <<https://doi.org/10.5281/zenodo.3956609>> (MGB code in
831 FORTRAN, MGB Input folder, post-processing code in MATLAB).

832

833 **References**

- 834 Aires, F. (2014). Combining Datasets of Satellite-Retrieved Products. Part I:
835 Methodology and Water Budget Closure. *Journal of Hydrometeorology*.
836 <https://doi.org/10.1175/jhm-d-13-0148.1>
- 837 Alkama, R., Decharme, B., Douville, H., Becker, M., Cazenave, A., Sheffield, J., et al.
838 (2010). Global evaluation of the ISBA-TRIP continental hydrological system. Part
839 I: Comparison to GRACE terrestrial water storage estimates and in situ river

840 discharges. *Journal of Hydrometeorology*. <https://doi.org/10.1175/2010JHM1211.1>

841 Asadzadeh Jarihani, A., Callow, J. N., Johansen, K., & Gouweleeuw, B. (2013).
842 Evaluation of multiple satellite altimetry data for studying inland water bodies and
843 river floods. *Journal of Hydrology*. <https://doi.org/10.1016/j.jhydrol.2013.09.010>

844 Baroni, G., Schalge, B., Rakovec, O., Kumar, R., Schüler, L., Samaniego, L., et al.
845 (2019). A Comprehensive Distributed Hydrological Modeling Intercomparison to
846 Support Process Representation and Data Collection Strategies. *Water Resources*
847 *Research*. <https://doi.org/10.1029/2018WR023941>

848 Bates, P. D., Horritt, M. S., & Fewtrell, T. J. (2010). A simple inertial formulation of
849 the shallow water equations for efficient two-dimensional flood inundation
850 modelling. *Journal of Hydrology*. <https://doi.org/10.1016/j.jhydrol.2010.03.027>

851 Beven, K. (2006). A manifesto for the equifinality thesis. In *Journal of Hydrology*.
852 <https://doi.org/10.1016/j.jhydrol.2005.07.007>

853 Beven, K., & Binley, A. (1992). The future of distributed models: Model calibration and
854 uncertainty prediction. *Hydrological Processes*.
855 <https://doi.org/10.1002/hyp.3360060305>

856 Blöschl, G., Bierkens, M. F. P., Chambel, A., Cudennec, C., Destouni, G., Fiori, A., et
857 al. (2019). Twenty-three Unsolved Problems in Hydrology (UPH)—A community
858 perspective. *Hydrological Sciences Journal*.
859 <https://doi.org/10.1080/02626667.2019.1620507>

860 Brêda, J. P. L. F., Paiva, R. C. D., Bravo, J. M., Passaia, O. A., & Moreira, D. M.
861 (2019). Assimilation of Satellite Altimetry Data for Effective River Bathymetry.
862 *Water Resources Research*. <https://doi.org/10.1029/2018wr024010>

863 Clark, M. P., Fan, Y., Lawrence, D. M., Adam, J. C., Bolster, D., Gochis, D. J., et al.
864 (2015). Improving the representation of hydrologic processes in Earth System
865 Models. *Water Resources Research*. <https://doi.org/10.1002/2015WR017096>

866 Collischonn, B., Collischonn, W., & Tucci, C. E. M. (2008). Daily hydrological
867 modeling in the Amazon basin using TRMM rainfall estimates. *Journal of*
868 *Hydrology*. <https://doi.org/10.1016/j.jhydrol.2008.07.032>

869 Collischonn, W., Allasia, D., da Silva, B. C., & Tucci, C. E. M. (2007). The MGB-IPH
870 model for large-scale rainfall-runoff modelling. *Hydrological Sciences Journal*.
871 <https://doi.org/10.1623/hysj.52.5.878>

872 Croke, B. F. W. (2009). Representing uncertainty in objective functions: Extension to
873 include the influence of serial correlation. In *18th World IMACS Congress and*
874 *MODSIM09 International Congress on Modelling and Simulation: Interfacing*
875 *Modelling and Simulation with Mathematical and Computational Sciences,*
876 *Proceedings*.

877 Crow, W. T., Wood, E. F., & Pan, M. (2003). Multiobjective calibration of land surface
878 model evapotranspiration predictions using streamflow observations and
879 spaceborne surface radiometric temperature retrievals. *Journal of Geophysical*
880 *Research D: Atmospheres*. <https://doi.org/10.1029/2002JD003292>

881 Dembele, M., Ceperley, N., Zwart, S.J., Salvadore, E., Mariethoz, G., Schaefli, B.
882 (2020). Potential of satellite and reanalysis evaporation datasets for hydrological
883 modelling under various model calibration strategies. *Advances in Water*
884 *Resources*. <https://doi.org/10.1016/j.advwatres.2020.103667>

885 Demirel, M. C., Mai, J., Mendiguren, G., Koch, J., Samaniego, L., & Stisen, S. (2018).
886 Combining satellite data and appropriate objective functions for improved spatial

887 pattern performance of a distributed hydrologic model. *Hydrology and Earth*
888 *System Sciences*. <https://doi.org/10.5194/hess-22-1299-2018>

889 Demirel, M. C., Özen, A., Orta, S., Toker, E., Demir, H. K., Ekmekcioglu, Ö., Taysi,
890 H., Eruçar, S., Sag, A. B., Sari, Ö., Tuncer, E., Hanci, H., Özcan, T. I., Erdem, H.,
891 Kosucu, M. M., Basakin, E. E., Ahmed, K., Anwar, A., Avcuoglu, M. B., Vanli,
892 Ö., Stisen, S., & Booij, M. J. (2019). Additional value of using satellite-based soil
893 moisture and two sources of groundwater data for hydrological model calibration.
894 *Water*. <https://doi.org/10.3390/w11102083>

895 Di Baldassarre, G., & Montanari, A. (2009). Uncertainty in river discharge
896 observations: A quantitative analysis. *Hydrology and Earth System Sciences*.
897 <https://doi.org/10.5194/hess-13-913-2009>

898 Duan, Q., Sorooshian, S., & Gupta, V. (1992). Effective and efficient global
899 optimization for conceptual rainfall–runoff models. *Water Resources Research*.
900 <https://doi.org/10.1029/91WR02985>

901 Fan, F. M., Buarque, D. C., Pontes, P. R. M., & Collischonn, W. (2015). Um mapa de
902 Unidades de Resposta Hidrológica para a América do Sul. *XXI Simpósio Brasileiro*
903 *de Recursos Hídricos*.

904 Fleischmann, A.S., Paiva, R.C.D., Collischonn, W., Siqueira, V.A., Paris, A., Moreira,
905 D.M., Papa, F., Bitar, A.A., Parrens, M., Aires, F. & Garambois, P.A. (2020).
906 Trade-offs between 1D and 2D regional river hydrodynamic models. *Water*
907 *Resources Research*. <https://doi.org/10.1029/2019WR026812>

908 Foglia, L., Hill, M. C., Mehl, S. W., & Burlando, P. (2009). Sensitivity analysis,
909 calibration, and testing of a distributed hydrological model using error-based
910 weighting and one objective function. *Water Resources Research*.

911 <https://doi.org/10.1029/2008WR007255>

912 Franks, S. W., Gineste, P., Beven, K. J., & Merot, P. (1998). On constraining the
913 predictions of a distributed model: The incorporation of fuzzy estimates of
914 saturated areas into the calibration process. *Water Resources Research*.
915 <https://doi.org/10.1029/97WR03041>

916 Gharari, S., Shafiei, M., Hrachowitz, M., Kumar, R., Fenicia, F., Gupta, H. V., &
917 Savenije, H. H. G. (2014). A constraint-based search algorithm for parameter
918 identification of environmental models. *Hydrology and Earth System Sciences*.
919 <https://doi.org/10.5194/hess-18-4861-2014>

920 Gomis-Cebolla, J., Jimenez, J. C., Sobrino, J. A., Corbari, C., & Mancini, M. (2019).
921 Intercomparison of remote-sensing based evapotranspiration algorithms over
922 amazonian forests. *International Journal of Applied Earth Observation and*
923 *Geoinformation*. <https://doi.org/10.1016/j.jag.2019.04.009>

924 Grimaldi, S., Schumann, G. J. P., Shokri, A., Walker, J. P., & Pauwels, V. R. N. (2019).
925 Challenges, Opportunities, and Pitfalls for Global Coupled Hydrologic-Hydraulic
926 Modeling of Floods. *Water Resources Research*.
927 <https://doi.org/10.1029/2018WR024289>

928 Gupta, H. V., Kling, H., Yilmaz, K. K., & Martinez, G. F. (2009). Decomposition of the
929 mean squared error and NSE performance criteria: Implications for improving
930 hydrological modelling. *Journal of Hydrology*.
931 <https://doi.org/10.1016/j.jhydrol.2009.08.003>

932 Haddeland, I., Skaugen, T., & Lettenmaier, D. P. (2006). Anthropogenic impacts on
933 continental surface water fluxes. *Geophysical Research Letters*.
934 <https://doi.org/10.1029/2006GL026047>

- 935 Hasler, N., & Avissar, R. (2007). What controls evapotranspiration in the Amazon
936 basin? *Journal of Hydrometeorology*. <https://doi.org/10.1175/JHM587.1>
- 937 Herman, M. R., Nejadhashemi, A. P., Abouali, M., Hernandez-suarez, S., Daneshvar,
938 F., Zhang, Z., et al. (2017). Evaluating the Role of Evapotranspiration Remote
939 Sensing Data in Improving Hydrological Modeling Predictability. *Journal of*
940 *Hydrology*. <https://doi.org/10.1016/j.jhydrol.2017.11.009>
- 941 Hess, L. L., Melack, J. M., Novo, E. M. L. M., Barbosa, C. C. F., & Gastil, M. (2003).
942 Dual-season mapping of wetland inundation and vegetation for the central Amazon
943 basin. *Remote Sensing of Environment*. <https://doi.org/10.1016/j.rse.2003.04.001>
- 944 Hodges, B. R. (2013). Challenges in continental river dynamics. *Environmental*
945 *Modelling and Software*. <https://doi.org/10.1016/j.envsoft.2013.08.010>
- 946 Holeman, J. N. (1968). The Sediment Yield of Major Rivers of the World. *Water*
947 *Resources Research*. <https://doi.org/10.1029/WR004i004p00737>
- 948 Houser, P. R., Shuttleworth, W. J., Famiglietti, J. S., Gupta, H. V., Syed, K. H., &
949 Goodrich, D. C. (1998). Integration of soil moisture remote sensing and hydrologic
950 modeling using data assimilation. *Water Resources Research*.
951 <https://doi.org/10.1029/1998WR900001>
- 952 Hrachowitz, M., Savenije, H. H. G., Blöschl, G., McDonnell, J. J., Sivapalan, M.,
953 Pomeroy, J. W., et al. (2013). A decade of Predictions in Ungauged Basins (PUB)-
954 a review. *Hydrological Sciences Journal*.
955 <https://doi.org/10.1080/02626667.2013.803183>
- 956 Huffman, G. J., Adler, R. F., Bolvin, D. T., Gu, G., Nelkin, E. J., Bowman, K. P., et al.
957 (2007). The TRMM Multisatellite Precipitation Analysis (TMPA): Quasi-global,

958 multiyear, combined-sensor precipitation estimates at fine scales. *Journal of*
959 *Hydrometeorology*. <https://doi.org/10.1175/JHM560.1>Jiang, D., & Wang, K.
960 (2019). The Role of Satellite-Based Remote Sensing in Improving Simulated
961 Streamflow: A Review. *Water*. <https://doi.org/10.3390/w11081615>

962 Junk, W. J. (1997). General Aspects of Floodplain Ecology with Special Reference to
963 Amazonian Floodplains. https://doi.org/10.1007/978-3-662-03416-3_1

964 Karthikeyan, L., Pan, M., Wanders, N., Kumar, D. N., & Wood, E. F. (2017). Four
965 decades of microwave satellite soil moisture observations: Part 2. Product
966 validation and inter-satellite comparisons. *Advances in Water Resources*.
967 <https://doi.org/10.1016/j.advwatres.2017.09.010>

968 Kerr, Y. H., Waldteufel, P., Wigneron, J. P., Martinuzzi, J. M., Font, J., & Berger, M.
969 (2001). Soil moisture retrieval from space: The Soil Moisture and Ocean Salinity
970 (SMOS) mission. *IEEE Transactions on Geoscience and Remote Sensing*.
971 <https://doi.org/10.1109/36.942551>

972 Kirchner, J. W. (2006). Getting the right answers for the right reasons: Linking
973 measurements, analyses, and models to advance the science of hydrology. *Water*
974 *Resources Research*. <https://doi.org/10.1029/2005WR004362>

975 Kittel, C., Nielsen, K., Tøttrup, C., & Bauer-Gottwein, P. (2018). Informing a
976 hydrological model of the Ogooué with multi-mission remote sensing data.
977 *Hydrology and Earth System Sciences*. <https://doi.org/10.5194/hess-22-1453-2018>

978 Koch, J., Demirel, M. C., & Stisen, S. (2018). The SPATial EFficiency metric (SPAEF):
979 Multiple-component evaluation of spatial patterns for optimization of hydrological
980 models. *Geoscientific Model Development*. [https://doi.org/10.5194/gmd-11-1873-](https://doi.org/10.5194/gmd-11-1873-2018)
981 2018

982 Koppa, A., Gebremichael, M., & Yeh, W. W. G. (2019). Multivariate calibration of
983 large scale hydrologic models: The necessity and value of a Pareto optimal
984 approach. *Advances in Water Resources*.
985 <https://doi.org/10.1016/j.advwatres.2019.06.005>

986 Kottek, M., Grieser, J., Beck, C., Rudolf, B., & Rubel, F. (2006). World map of the
987 Köppen-Geiger climate classification updated. *Meteorologische Zeitschrift*. [https://](https://doi.org/10.1127/0941-2948/2006/0130)
988 doi.org/10.1127/0941-2948/2006/0130

989 Lambin, J., Morrow, R., Fu, L. L., Willis, J. K., Bonekamp, H., Lillibridge, J., et al.
990 (2010). The OSTM/Jason-2 Mission. *Marine Geodesy*.
991 <https://doi.org/10.1080/01490419.2010.491030>

992 Lee, H., Jung, H. C., Yuan, T., Beighley, R. E., & Duan, J. (2014). Controls of
993 Terrestrial Water Storage Changes Over the Central Congo Basin Determined by
994 Integrating PALSAR ScanSAR, Envisat Altimetry, and GRACE Data. In *Remote*
995 *Sensing of the Terrestrial Water Cycle*.
996 <https://doi.org/10.1002/9781118872086.ch7>

997 Lettenmaier, D. P., Alsdorf, D., Dozier, J., Huffman, G. J., Pan, M., & Wood, E. F.
998 (2015). Inroads of remote sensing into hydrologic science during the WRR era.
999 *Water Resources Research*. <https://doi.org/10.1002/2015WR017616>

1000 Li, Y., Grimaldi, S., Pauwels, V. R. N., & Walker, J. P. (2018). Hydrologic model
1001 calibration using remotely sensed soil moisture and discharge measurements: The
1002 impact on predictions at gauged and ungauged locations. *Journal of Hydrology*.
1003 <https://doi.org/10.1016/j.jhydrol.2018.01.013>

1004 Liang, X., Lettenmaier, D. P., Wood, E. F., & Burges, S. J. (1994). A simple
1005 hydrologically based model of land surface water and energy fluxes for general

1006 circulation models. *Journal of Geophysical Research*.
1007 <https://doi.org/10.1029/94jd00483>

1008 Lo, M. H., Famiglietti, J. S., Yeh, P. J. F., & Syed, T. H. (2010). Improving parameter
1009 estimation and water table depth simulation in a land surface model using GRACE
1010 water storage and estimated base flow data. *Water Resources Research*.
1011 <https://doi.org/10.1029/2009WR007855>

1012 López, P. L., Sutanudjaja, E. H., Schellekens, J., Sterk, G., & Bierkens, M. F. P. (2017).
1013 Calibration of a large-scale hydrological model using satellite-based soil moisture
1014 and evapotranspiration products. *Hydrology and Earth System Sciences*.
1015 <https://doi.org/10.5194/hess-21-3125-2017>

1016 Maeda, E. E., Ma, X., Wagner, F. H., Kim, H., Oki, T., Eamus, D., & Huete, A. (2017).
1017 Evapotranspiration seasonality across the Amazon Basin. *Earth System Dynamics*.
1018 <https://doi.org/10.5194/esd-8-439-2017>

1019 Manfreda, S., Mita, L., Dal Sasso, S. F., Samela, C., & Mancusi, L. (2018). Exploiting
1020 the use of physical information for the calibration of a lumped hydrological model.
1021 *Hydrological Processes*. <https://doi.org/10.1002/hyp.11501>

1022 Maurer, E. P., Adam, J. C., & Wood, A. W. (2009). Climate model based consensus on
1023 the hydrologic impacts of climate change to the Rio Lempa basin of Central
1024 America. *Hydrology and Earth System Sciences*. [https://doi.org/10.5194/hess-13-](https://doi.org/10.5194/hess-13-183-2009)
1025 183-2009

1026 Milzow, C., Krogh, P. E., & Bauer-Gottwein, P. (2011). Combining satellite radar
1027 altimetry, SAR surface soil moisture and GRACE total storage changes for
1028 hydrological model calibration in a large poorly gauged catchment. *Hydrology and*
1029 *Earth System Sciences*. <https://doi.org/10.5194/hess-15-1729-2011>

1030 Mitchell, K. E., Lohmann, D., Houser, P. R., Wood, E. F., Schaake, J. C., Robock, A.,
1031 et al. (2004). The multi-institution North American Land Data Assimilation
1032 System (NLDAS): Utilizing multiple GCIP products and partners in a continental
1033 distributed hydrological modeling system. *Journal of Geophysical Research D:
1034 Atmospheres*. <https://doi.org/10.1029/2003JD003823>

1035 Montanari, A., & Koutsoyiannis, D. (2014). Modeling and mitigating natural hazards:
1036 Stationarity is immortal! *Water Resources Research*.
1037 <https://doi.org/10.1002/2014WR016092>

1038 Motovilov, Y. G., Gottschalk, L., Engeland, K., & Rodhe, A. (1999). Validation of a
1039 distributed hydrological model against spatial observations. *Agricultural and
1040 Forest Meteorology*. [https://doi.org/10.1016/S0168-1923\(99\)00102-1](https://doi.org/10.1016/S0168-1923(99)00102-1)

1041 Mu, Q., Zhao, M., & Running, S. W. (2011). Improvements to a MODIS global
1042 terrestrial evapotranspiration algorithm. *Remote Sensing of Environment*.
1043 <https://doi.org/10.1016/j.rse.2011.02.019>

1044 Naz, B. S., Frans, C. D., Clarke, G. K. C., Burns, P., & Lettenmaier, D. P. (2014).
1045 Modeling the effect of glacier recession on streamflow response using a coupled
1046 glacio-hydrological model. *Hydrology and Earth System Sciences*.
1047 <https://doi.org/10.5194/hess-18-787-2014>

1048 Neal, J.C., Odoni, N. A., Trigg, M.A., Freer, J. E., Garcia-Pintado, J., & Mason, D. C.
1049 (2015). Efficient incorporation of channel cross-section geometry uncertainty into
1050 regional and global scale flood inundation models. *Journal of Hydrology*.
1051 <https://doi.org/10.1016/j.jhydrol.2015.07.026>

1052 Neal, J., Schumann, G., & Bates, P. (2012). A subgrid channel model for simulating
1053 river hydraulics and floodplain inundation over large and data sparse areas. *Water*

1054 *Resources Research*. <https://doi.org/10.1029/2012WR012514>

1055 Nearing, G. S., Tian, Y., Gupta, H. V., Clark, M. P., Harrison, K. W., & Weijs, S. V.
1056 (2016). A philosophical basis for hydrological uncertainty. *Hydrological Sciences*
1057 *Journal*. <https://doi.org/10.1080/02626667.2016.1183009>

1058 Nepstad, D. C., De Carvalho, C. R., Davidson, E. A., Jipp, P. H., Lefebvre, P. A.,
1059 Negreiros, G. H., et al. (1994). The role of deep roots in the hydrological and
1060 carbon cycles of Amazonian forests and pastures. *Nature*.
1061 <https://doi.org/10.1038/372666a0>

1062 New, M., Hulme, M., & Jones, P. (2000). Representing twentieth-century space-time
1063 climate variability. Part II: Development of 1901-96 monthly grids of terrestrial
1064 surface climate. *Journal of Climate*. [https://doi.org/10.1175/1520-](https://doi.org/10.1175/1520-0442(2000)013<2217:RTCSTC>2.0.CO;2)
1065 [0442\(2000\)013<2217:RTCSTC>2.0.CO;2](https://doi.org/10.1175/1520-0442(2000)013<2217:RTCSTC>2.0.CO;2)

1066 Nijzink, R. C., Almeida, S., Pechlivanidis, I. G., Capell, R., Gustafssons, D., Arheimer,
1067 B., et al. (2018). Constraining Conceptual Hydrological Models With Multiple
1068 Information Sources. *Water Resources Research*.
1069 <https://doi.org/10.1029/2017WR021895>

1070 O'Loughlin, F. E., Paiva, R. C. D., Durand, M., Alsdorf, D. E., & Bates, P. D. (2016). A
1071 multi-sensor approach towards a global vegetation corrected SRTM DEM product.
1072 *Remote Sensing of Environment*. <https://doi.org/10.1016/j.rse.2016.04.018>

1073 Paiva, R. C.D., Collischonn, W., Bonnet, M. P., De Gonçalves, L. G. G., Calmant, S.,
1074 Getirana, A., & Santos Da Silva, J. (2013). Assimilating in situ and radar altimetry
1075 data into a large-scale hydrologic-hydrodynamic model for streamflow forecast in
1076 the Amazon. *Hydrology and Earth System Sciences*. [https://doi.org/10.5194/hess-](https://doi.org/10.5194/hess-17-2929-2013)
1077 [17-2929-2013](https://doi.org/10.5194/hess-17-2929-2013)

- 1078 Paiva, R. C.D., Collischonn, W., & Tucci, C. E. M. (2011). Large scale hydrologic and
1079 hydrodynamic modeling using limited data and a GIS based approach. *Journal of*
1080 *Hydrology*. <https://doi.org/10.1016/j.jhydrol.2011.06.007>
- 1081 Paiva, R. C. D., Buarque, D. C., Collischonn, W., Bonnet, M. P., Frappart, F., Calmant,
1082 S., & Bulhões Mendes, C. A. (2013). Large-scale hydrologic and hydrodynamic
1083 modeling of the Amazon River basin. *Water Resources Research*.
1084 <https://doi.org/10.1002/wrcr.20067>
- 1085 Pan, M., & Wood, E. F. (2006). Data assimilation for estimating the terrestrial water
1086 budget using a constrained ensemble Kalman filter. *Journal of Hydrometeorology*.
1087 <https://doi.org/10.1175/JHM495.1>
- 1088 Pan, S., Liu, L., Bai, Z., & Xu, Y. P. (2018). Integration of remote sensing
1089 evapotranspiration into multi-objective calibration of distributed hydrology-soil-
1090 vegetation model (DHSVM) in a humid region of China. *Water (Switzerland)*.
1091 <https://doi.org/10.3390/w10121841>
- 1092 Pan, S., Pan, N., Tian, H., Friedlingstein, P., Sitch, S., Shi, H., Arora, V.K., Haverd, V.,
1093 Jain, A.K., Kato, E., Lienert, S., Lombardozzi, D., Nabel, J.E.M.S., Ottlé, C.,
1094 Poulter, B., Zaehle, S., Running, S.W. (2020). Evaluation of global terrestrial
1095 evapotranspiration using state-of-the-art approaches in remote sensing, machine
1096 learning and land surface modeling. *Hydrol. Earth Syst. Sci*.
1097 <https://doi.org/10.5194/hess-24-1485-2020>
- 1098 Pathiraja, S., Marshall, L., Sharma, A., & Moradkhani, H. (2016). Hydrologic modeling
1099 in dynamic catchments: A data assimilation approach. *Water Resources Research*.
1100 <https://doi.org/10.1002/2015WR017192>
- 1101 Pellet, V., Aires, F., Munier, S., Fernández Prieto, D., Jordá, G., Arnaud Dorigo, W., et

1102 al. (2019). Integrating multiple satellite observations into a coherent dataset to
1103 monitor the full water cycle - Application to the Mediterranean region. *Hydrology*
1104 *and Earth System Sciences*. <https://doi.org/10.5194/hess-23-465-2019>

1105 Peña-Arancibia, J. L., Zhang, Y., Pagendam, D. E., Viney, N. R., Lerat, J., van Dijk, A.
1106 I. J. M., et al. (2015). Streamflow rating uncertainty: Characterisation and impacts
1107 on model calibration and performance. *Environmental Modelling and Software*.
1108 <https://doi.org/10.1016/j.envsoft.2014.09.011>

1109 Poméon, T., Diekkrüger, B., & Kumar, R. (2018). Computationally efficient
1110 multivariate calibration and validation of a grid-based hydrologic model in sparsely
1111 gauged West African river basins. *Water (Switzerland)*.
1112 <https://doi.org/10.3390/w10101418>

1113 Pontes, P. R. M., Fan, F. M., Fleischmann, A. S., de Paiva, R. C. D., Buarque, D. C.,
1114 Siqueira, V. A., et al. (2017). MGB-IPH model for hydrological and hydraulic
1115 simulation of large floodplain river systems coupled with open source GIS.
1116 *Environmental Modelling and Software*.
1117 <https://doi.org/10.1016/j.envsoft.2017.03.029>

1118 Rajib, M. A., Merwade, V., & Yu, Z. (2016). Multi-objective calibration of a hydrologic
1119 model using spatially distributed remotely sensed/in-situ soil moisture. *Journal of*
1120 *Hydrology*. <https://doi.org/10.1016/j.jhydrol.2016.02.037>

1121 Rakovec, O., Kumar, R., Attinger, S., & Samaniego, L. (2016). Improving the realism
1122 of hydrologic model functioning through multivariate parameter estimation. *Water*
1123 *Resources Research*. <https://doi.org/10.1002/2016WR019430>

1124 Reichle, R. H., McLaughlin, D. B., & Entekhabi, D. (2002). Hydrologic data
1125 assimilation with the ensemble Kalman filter. *Monthly Weather Review*.

- 1126 [https://doi.org/10.1175/1520-0493\(2002\)130<0103:HDAWTE>2.0.CO;2](https://doi.org/10.1175/1520-0493(2002)130<0103:HDAWTE>2.0.CO;2)
- 1127 Rosenqvist, A., Shimada, M., Ito, N., & Watanabe, M. (2007). ALOS PALSAR: A
1128 pathfinder mission for global-scale monitoring of the environment. In *IEEE*
1129 *Transactions on Geoscience and Remote Sensing*.
1130 <https://doi.org/10.1109/TGRS.2007.901027>
- 1131 Samaniego, L., Kumar, R., & Attinger, S. (2010). Multiscale parameter regionalization
1132 of a grid-based hydrologic model at the mesoscale. *Water Resources Research*.
1133 <https://doi.org/10.1029/2008WR007327>
- 1134 Schattan, P., Schwaizer, G., Schöber, J., & Achleitner, S. (2020). The complementary
1135 value of cosmic-ray neutron sensing and snow covered area products for snow
1136 hydrological modelling. *Remote Sensing of Environment*.
1137 <https://doi.org/10.1016/j.rse.2019.111603>
- 1138 Schneider, R., Nygaard Godiksen, P., Villadsen, H., Madsen, H., & Bauer-Gottwein, P.
1139 (2017). Application of CryoSat-2 altimetry data for river analysis and modelling.
1140 *Hydrology and Earth System Sciences*. <https://doi.org/10.5194/hess-21-751-2017>
- 1141 Schumacher, M., Forootan, E., van Dijk, A. I. J. M., Müller Schmied, H., Crosbie, R. S.,
1142 Kusche, J., & Döll, P. (2018). Improving drought simulations within the Murray-
1143 Darling Basin by combined calibration/assimilation of GRACE data into the
1144 WaterGAP Global Hydrology Model. *Remote Sensing of Environment*.
1145 <https://doi.org/10.1016/j.rse.2017.10.029>
- 1146 Semenova, O., & Beven, K. (2015). Barriers to progress in distributed hydrological
1147 modelling. *Hydrological Processes*. <https://doi.org/10.1002/hyp.10434>
- 1148 Shafii, M., & Tolson, B. A. (2015). Optimizing hydrological consistency by

1149 incorporating hydrological signatures into model calibration objectives. *Water*
1150 *Resources Research*. <https://doi.org/10.1002/2014WR016520>

1151 Silvestro, F., Gabellani, S., Rudari, R., Delogu, F., Laiolo, P., & Boni, G. (2015).
1152 Uncertainty reduction and parameter estimation of a distributed hydrological
1153 model with ground and remote-sensing data. *Hydrology and Earth System*
1154 *Sciences*. <https://doi.org/10.5194/hess-19-1727-2015>

1155 Siqueira, V., Fleischmann, A., Jardim, P., Fan, F., & Collischonn, W. (2016). IPH-
1156 Hydro Tools: a GIS coupled tool for watershed topology acquisition in an open-
1157 source environment. *Revista Brasileira de Recursos Hídricos*.
1158 <https://doi.org/10.21168/rbrh.v21n1.p274-287>

1159 Siqueira, V. A., Paiva, R. C. D., Fleischmann, A. S., Fan, F. M., Ruhoff, A. L., Pontes,
1160 P. R. M., et al. (2018). Toward continental hydrologic-hydrodynamic modeling in
1161 South America. *Hydrology and Earth System Sciences*.
1162 <https://doi.org/10.5194/hess-22-4815-2018>

1163 Sivapalan, M., Takeuchi, K., Franks, S. W., Gupta, V. K., Karambiri, H., Lakshmi, V.,
1164 et al. (2003). IAHS Decade on Predictions in Ungauged Basins (PUB), 2003-2012:
1165 Shaping an exciting future for the hydrological sciences. *Hydrological Sciences*
1166 *Journal*. <https://doi.org/10.1623/hysj.48.6.857.51421>

1167 Sun, W., Ishidaira, H., & Bastola, S. (2012). Calibration of hydrological models in
1168 ungauged basins based on satellite radar altimetry observations of river water level.
1169 *Hydrological Processes*. <https://doi.org/10.1002/hyp.8429>

1170 Sun, W., Fan, J., Wang, G., Ishidaira, H., Bastola, S., Yu, J., et al. (2018). Calibrating a
1171 hydrological model in a regional river of the Qinghai–Tibet plateau using river
1172 water width determined from high spatial resolution satellite images. *Remote*

- 1173 *Sensing of Environment*. <https://doi.org/10.1016/j.rse.2018.05.020>
- 1174 Sun, W. C., Ishidaira, H., & Bastola, S. (2010). Towards improving river discharge
1175 estimation in ungauged basins: Calibration of rainfall-runoff models based on
1176 satellite observations of river flow width at basin outlet. *Hydrology and Earth
1177 System Sciences*. <https://doi.org/10.5194/hess-14-2011-2010>
- 1178 Tapley, B. D., Bettadpur, S., Ries, J. C., Thompson, P. F., & Watkins, M. M. (2004).
1179 GRACE measurements of mass variability in the Earth system. *Science*.
1180 <https://doi.org/10.1126/science.1099192>
- 1181 Tarpanelli, A., Brocca, L., Melone, F., & Moramarco, T. (2013). Hydraulic modelling
1182 calibration in small rivers by using coarse resolution synthetic aperture radar
1183 imagery. *Hydrological Processes*. <https://doi.org/10.1002/hyp.9550>
- 1184 Teutschbein, C., & Seibert, J. (2012). Bias correction of regional climate model
1185 simulations for hydrological climate-change impact studies: Review and evaluation
1186 of different methods. *Journal of Hydrology*.
1187 <https://doi.org/10.1016/j.jhydrol.2012.05.052>
- 1188 Vrugt, J. A., Diks, C. G. H., Gupta, H. V., Bouten, W., & Verstraten, J. M. (2005).
1189 Improved treatment of uncertainty in hydrologic modeling: Combining the
1190 strengths of global optimization and data assimilation. *Water Resources Research*.
1191 <https://doi.org/10.1029/2004WR003059>
- 1192 Wagener, T., McIntyre, N., Lees, M. J., Wheater, H. S., & Gupta, H. V. (2003).
1193 Towards reduced uncertainty in conceptual rainfall-runoff modelling: Dynamic
1194 identifiability analysis. *Hydrological Processes*. <https://doi.org/10.1002/hyp.1135>
- 1195 Wambura, F. J., Dietrich, O., & Lischeid, G. (2018). Improving a distributed

1196 hydrological model using evapotranspiration-related boundary conditions as
1197 additional constraints in a data-scarce river basin. *Hydrological Processes*.
1198 <https://doi.org/10.1002/hyp.11453>

1199 Werth, S., & Güntner, A. (2010). Calibration analysis for water storage variability of the
1200 global hydrological model WGHM. *Hydrology and Earth System Sciences*. [https://](https://doi.org/10.5194/hess-14-59-2010)
1201 doi.org/10.5194/hess-14-59-2010

1202 Werth, S., Güntner, A., Petrovic, S., & Schmidt, R. (2009). Integration of GRACE mass
1203 variations into a global hydrological model. *Earth and Planetary Science Letters*.
1204 <https://doi.org/10.1016/j.epsl.2008.10.021>

1205 Willem Vervoort, R., Miechels, S. F., van Ogtrop, F. F., & Guillaume, J. H. A. (2014).
1206 Remotely sensed evapotranspiration to calibrate a lumped conceptual model:
1207 Pitfalls and opportunities. *Journal of Hydrology*.
1208 <https://doi.org/10.1016/j.jhydrol.2014.10.034>

1209 Winsemius, H. C., G. Savenije, H. H., & M. Bastiaanssen, W. G. (2008). Constraining
1210 model parameters on remotely sensed evaporation: Justification for distribution in
1211 ungauged basins? *Hydrology and Earth System Sciences*.
1212 <https://doi.org/10.5194/hess-12-1403-2008>

1213 Xu, C. Y., Widén, E., & Halldin, S. (2005). Modelling hydrological consequences of
1214 climate change - Progress and challenges. *Advances in Atmospheric Sciences*.
1215 <https://doi.org/10.1007/BF02918679>

1216 Xu, X., Li, J., & Tolson, B. A. (2014). Progress in integrating remote sensing data and
1217 hydrologic modeling. *Progress in Physical Geography*.
1218 <https://doi.org/10.1177/0309133314536583>

1219 Yamazaki, D., Kanae, S., Kim, H., & Oki, T. (2011). A physically based
1220 description of floodplain inundation dynamics in a global river routing
1221 model. *Water Resources Research*. <https://doi.org/10.1029/2010WR009726>

1222 Yapo, P. O., Gupta, H. V., & Sorooshian, S. (1998). Multi-objective global optimization
1223 for hydrologic models. *Journal of Hydrology*. <https://doi.org/10.1016/S0022->
1224 1694(97)00107-8

1225 Zajac, Z., Revilla-Romero, B., Salamon, P., Burek, P., Hirpa, F., & Beck, H. (2017).
1226 The impact of lake and reservoir parameterization on global streamflow
1227 simulation. *Journal of Hydrology*. <https://doi.org/10.1016/j.jhydrol.2017.03.022>

1228 Zink, M., Mai, J., Cuntz, M., & Samaniego, L. (2018). Conditioning a Hydrologic
1229 Model Using Patterns of Remotely Sensed Land Surface Temperature. *Water*
1230 *Resources Research*. <https://doi.org/10.1002/2017WR021346>

1231